QUANTIFYING URBAN DAMAGE DUE TO SLOW-MOVING LANDSLIDES: A MULTI-INSTRUMENT AND MULTI-DISCIPLINARY APPROACH

DAVIDE NOTTI[1], MARTINA CIGNETTI[1], DAVIDE CARDONE[1], DARIO PEDUTO[2], GIANFRANCO NICODEMO[2], DAVIDE LUONGO[2], ROSSELLA BOVOLENTA[3], BIANCA FEDERICI[3], DIEGO REALE[4], SIMONA VERDE[4], FABIANA CALÒ[4], EUGENIO SANSOSTI[4], GIANFRANCO FORNARO[4], DANIELE GIORDAN[1]

[1] *National Research Council of Italy, Research Institute for Geo-Hydrological Protection (CNR-IRPI),Torino, Italy, daniele.giordan@irpi.cnr.it*

[2] *Department of Civil Engineering, University of Salerno, Fisciano, Italy, dpeduto@unisa.it*

[3] *Department of Civil, Chemical and Environmental Engineering, University of Genova, Genova, Italy, rossella.bovolenta@unige.it*

[4] *National Research Council of Italy, Institute for Electromagnetic Sensing of the Environment (CNR-IREA), Napoli, Italy, fornaro.g@irea.cnr.it*

Introduction

Slow-moving landslides are impactful phenomena in mountainous regions, affecting buildings and infrastructure with critical economic and social consequences. Nowadays, the use of integrative approaches is increasing to obtain a comprehensive assessment of these complex phenomena, as well as the evaluation of their impact (Cardone et al., 2023; Notti et al., 2021; Peduto et al., 2018). This strategy allows for a proper definition of risk mitigation policies, ensuring the safety of citizens and urban areas (Cignetti et al., 2022; Peduto et al., 2021). In this context, we introduce a methodology to temporally and spatially characterize large slow-moving landslides and assess the related evolution and impact on anthropic elements, through the combined analysis of multi-source and multi-sensor data. We apply this methodology to Mendatica, Arroscia Valley (Ligurian Alps, northwestern Italy), affected by large relict and dormant landslides, with an active landslide portion impacting the village (Pepe et al., 2021). By exploiting the progressive installation of on-site instruments associated with SAR data processing and damage level investigation on buildings, we operated an overall historical reconstruction of the evolution of this slow-movement phenomenon and related impact.

Methodology

The proposed methodology consists of a multi-instrument and multi-disciplinary approach that merges geological-geomorphological ancillary data, on-site instruments measurements, satellite monitoring and building damage survey to improve the comprehension of the relation between the morphology and kinematics of landslides and the induced effects on the built-up environment (Figure 1).

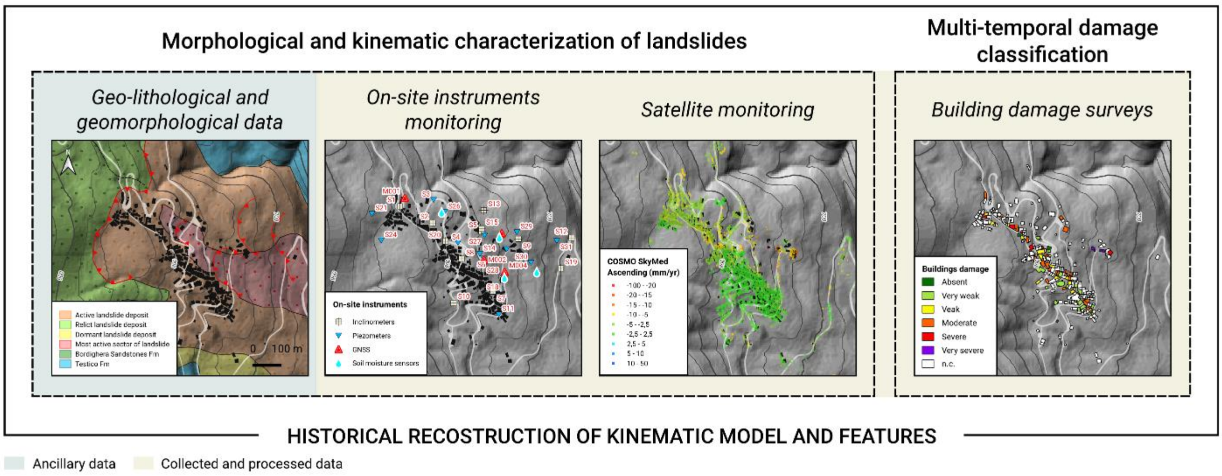

Figure 1. Outline of the materials and methodology used.

An investigation and collection of multi-source and multi-temporal data was carried out. Ancillary data were derived from national and regional web-portals (Federici et al., 2007; Trigila et al., 2008). In situ monitoring data, i.e., soil moisture measures (Bovolenta et al., 2020), borehole data (inclinometer and piezometer), and GNSS were analysed. An integration with SAR satellite images collected, processed and interpreted, including the multi-frequency SAR data (X-, C- and L-bands) and multi-temporal ranging in 2014-2022 (Noviello et al., 2020), has been carried out. A damage severity map was obtained from a field survey of buildings and infrastructures. Damage severity classification was performed using a ranking scale of five classes, ranging from 0 (negligible damage) to 5 (very severe damage) (Peduto et al., 2017). The kinematic characterization coupled with damage classification allows us to investigate the influence of landslide movement, allowing a complete reconstruction of its evolution and impact.

Results

Preliminary results reveal that most of the buildings examined during the field survey have negligible damage levels in the portion of the village built on relict/dormant landslides. In contrast, diffuse moderate to severe damage is located in the reactivations in the northeast sector. Buildings with very severe damage are concentrated in the eastern sector of the Mendatica village, which corresponds to the area with the most significant landslide activity. Within this sector, COSMO-SkyMed line-of-sight deformation registered the highest values, exceeding 10 mm/yr. In general, there is a good match between the CSK measurements and the building damage severity levels recorded during the last field survey in May 2023 (Figure 2). Nevertheless, many interacting factors (object of ongoing study) create a heterogeneous damage pattern. Field measurements of soil water content and piezometric level, automatically processed within the LAndslide Monitoring and Predicting (LAMP) system (Viaggio et al., 2022), confirmed critical areas of rain-induced slope instability, especially at Borgata Piano and allowed real-time analysis of landslide susceptibility with which urban damage is related.

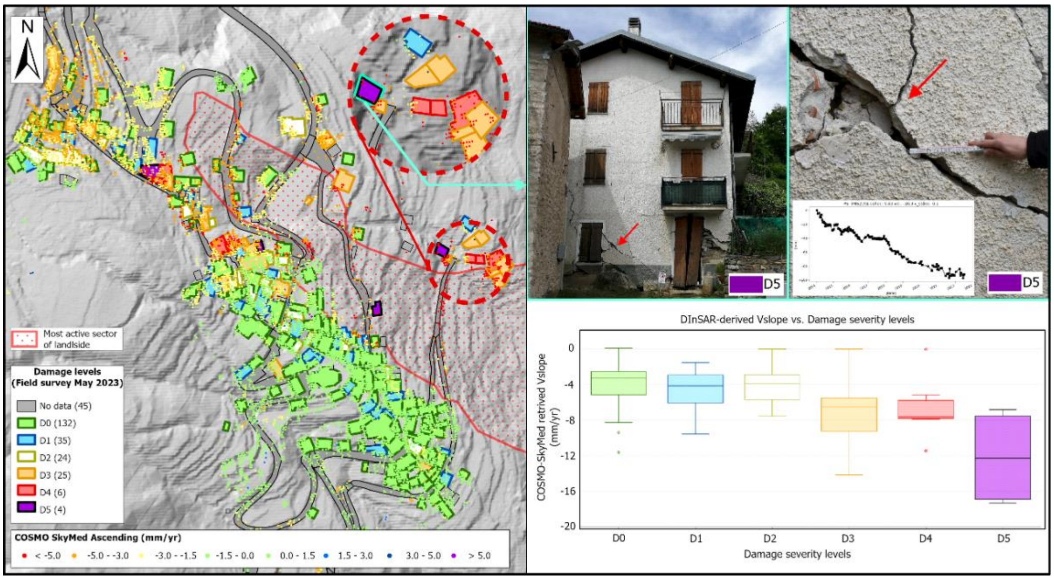

Figure 2. Comparison of damage levels recorded by the field survey and deformation data from CSK ascending geometry.

Conclusion

The multidisciplinary approach proposed is a way to understand better the complex relationship between landslide kinematics and damage to buildings and infrastructure. The coupled information given by the spatial diffuse monitoring given by multi-temporal SAR, combined with in-depth measures (e.g., moisture and inclinometers), is essential for understanding kinematics. At the same time, a detailed and rigorous building damage survey (engineering approach) helps to assess the effect of landslide movement. The same approach could be a model for many slow-moving landslides that affect villages in many mountain areas, representing a suitable approach in risk assessment and proper land use planning.

References

Bovolenta, R., Iacopino, A., Passalacqua, R., Federici, B., 2020. Field Measurements of Soil Water Content at Shallow Depths for Landslide Monitoring. Geosciences 10, 409. https://doi.org/10.3390/geosciences10100409

Cardone, D., Cignetti, M., Notti, D., Godone, D., Giordan, D., Calò, F., Verde, S., Reale, D., Sansosti, E., Fornaro, G., 2023. Slope-Scale Evolution Categorization of Deep-Seated Slope Deformation Phenomena with Sentinel-1 Data. Remote Sensing 15, 5440. https://doi.org/10.3390/rs15235440

Cignetti, M., Godone, D., Notti, D., Zucca, F., Meisina, C., Bordoni, M., Pedretti, L., Lanteri, L., Bertolo, D., Giordan, D., 2022. Damage to anthropic elements estimation due to large slope instabilities through multi-temporal A-DInSAR analysis. Natural Hazards 1–30. https://doi.org/10.1007/S11069-022-05655-7/FIGURES/15

Federici, P.R., Chelli, A., Biagioni, F., Rapetti, F., 2007. Atlante dei centri abitati instabili della Liguria - IV Provincia di Imperia. Regione Liguria pag. 163.

Notti, D., Wrzesniak, A., Dematteis, N., Lollino, P., Fazio, N.L., Zucca, F., Giordan, D., 2021. A multidisciplinary investigation of deep-seated landslide reactivation triggered by an extreme rainfall event: a case study of the Monesi di Mendatica landslide, Ligurian Alps. Landslides 18, 2341–2365. https://doi.org/10.1007/s10346-021-01651-3

Noviello, C., Peduto, D., Verde, S., Zamparelli, V., Fornaro, G., Pauciullo, A., Reale, D., Nicodemo, G., Ferlisi, S., Gulla, G., 2020. Monitoring Buildings at Landslide Risk With SAR: A Methodology Based on the Use of Multipass Interferometric Data. IEEE Geoscience and Remote Sensing Magazine 8, 91–119. https://doi.org/10.1109/MGRS.2019.2963140

Peduto, D., Ferlisi, S., Nicodemo, G., Reale, D., Pisciotta, G., Gullà, G., 2017. Empirical fragility and vulnerability curves for buildings exposed to slow-moving landslides at medium and large scales. Landslides 14, 1993–2007. https://doi.org/10.1007/s10346-017-0826-7

Peduto, D., Nicodemo, G., Caraffa, M., Gullà, G., 2018. Quantitative analysis of consequences to masonry buildings interacting with slow-moving landslide mechanisms: a case study. Landslides 15, 2017–2030. https://doi.org/10.1007/s10346-018-1014-0

Peduto, D., Santoro, M., Aceto, L., Borrelli, L., Gullà, G., 2021. Full integration of geomorphological, geotechnical, A-DInSAR and damage data for detailed geometric-kinematic features of a slow-moving landslide in urban area. Landslides 18, 807–825. https://doi.org/10.1007/s10346-020-01541-0

Pepe, G., Cevasco, A., Piazza, M., Macciò, R., Arrighetti, F., Casagli, N., 2021. On the efficiency and effectiveness of automatic deep drainage systems during an extreme rainfall event: the Mendatica landslide case study (western Liguria, Italy). Landslides 18, 3799–3820. https://doi.org/10.1007/s10346-021-01740-3

Trigila, A., Iadanza, C., Spizzichino, D., 2008. IFFI Project (Italian landslide inventory) and risk assessment, in: First World Landslide Forum. pp. 18–21.

Viaggio, S., Iacopino, A., Bovolenta, R., Federici, B., 2022. Landslide susceptibility assessment: soil moisture monitoring data processed by an automatic procedure in GIS for 3D description of the soil shear strength. The International Archives of the Photogrammetry, Remote Sensing and Spatial Information Sciences XLVIII-4-W1-2022, 517–523. https://doi.org/10.5194/isprs-archives-XLVIII-4-W1-2022-517-2022

COSMO-SkyMed and SAOCOM images have been provided by ASI under license to use agreements in the framework of the MEFISTO Project (ASI contract n. 2021-10-U.0 CUP F65F21000630005). Product produced from Original SAOCOM Product - ©CONAE – Comisión Nacional de Actividades Espaciales (2021).

SINKHOLE HAZARD ASSESSMENT ON DOLOMITE LAND: A CASE STUDY OF KHUTSONG NORTH, CARLETONVILLE – GAUTENG PROVINCE IN SOUTH AFRICA

SIFISO NGUBELANGA[1], GOODMAN CHILIZA[2], BONGANI MSANE[3], MAKGARI SEBESHO[4]

[1] *Council for Geoscience, South Africa, sngubelanga@geoscience.org.za*

[2] *Council for Geoscience, South Africa, gchiliza@geoscience.org.za*

[3] *Council for Geoscience, South Africa, bmsane@geoscience.org.za*

[4] *Council for Geoscience, South Africa, msebesho@geoscience.org.za*

Introduction

Hazard assessment is a key component within the broader risk analysis process, including the risk analysis for geological hazards. Jennings (1966a) described hazards on dolomite land as taking place in one of two ways, i.e. as a gradual or caving "subsidence" or a rapid and catastrophic subsidence defined as "sinkhole". In his analysis of the problem of building on dolomite, Jennings (1966a) concluded that any structure built on dolomitic subsoil, be it house, office block, industrial plant, road, railway line, dam, etc. might be exposed to danger of subsidence. Variability of ground conditions in karst terrains, nature of earth materials and urbanization are critical factors contributing to the problem.

Increased urbanization of dolomite "karst" land around major metropolitan (City of Ekurhuleni, City of Johannesburg and City of Tshwane) areas of the Gauteng Province, have resulted in densely populated townships like Khutsong, thereby exacerbating the risk posed by dolomite related ground instability events. These events occur primarily due to the loss of roof support and eventual collapse of the final roof arch into subsurface cavities. In South Africa, sinkholes and subsidences do occur, and is mostly ascribed to concentrated ingress of water eroding material into subsurface cavities, or regional groundwater lowering or dewatering resulting in loss of roof support of the cavity (Dippenaar et al., 2019). The frequency and severity of the problem is much increased in areas where the water table is lowered (Jennings et al., 1965), or where it naturally occurs at greater depths.

The greatest challenge in hazard assessment is represented by lack of any data, poor quality or limited availability because only the most destructive events are captured in public media platforms including literature. It is in this context that the research team selected three of the most destructive events for analysis and linked these to the natural setting and influence of the anthropogenic activities to determine (1) the hazard rating and (2) estimate the probability (using a formular by Kirsten *et al.*, 2014) of any sinkhole event causing damage to a house/ building, road and water or sewer pipeline.

Methods

Hazard assessment process requires that complete data sets be available to characterize the identified hazard. Lack of any data, poor quality or limited availability of crucial information in the data set may prohibit a credible hazard assessment process regardless of the adopted method. The method for dolomite land hazard assessment in South Africa is described by Buttrick *et al*., (2001), expanded in Buttrick *et al*., (2011), and incorporated into the South African National Standard (SANS) 1936. It requires that geological, geotechnical, geophysical and geohydrological data gathered during site investigation be collated and analysed to formulate a perspective on the stability of a dolomite site.

Subsequently, this method requires that a site be zoned in terms of inherent hazard class (IHC – 1 to 8), which is ultimately expressed in three broad inherent hazard categories, i.e. low, medium, and high. Buttrick *et al*., (2001), also defined sinkhole diameter of surface manifestation into four sizes, i.e. small (<2m), medium (2-5m), large (5-15m) and very large (>15m).

Results

The results of the current study and the discernible trends or observation maybe summarized as follows:

- IHC and zonation – the study area is dominated by high hazard with pockets of medium hazard.
- Events distribution and data quality – the study area is dominated by large to very-large (72%) size events and 78% of the sinkhole data lack details on the cause of events.
- Determination of hazard rating – in confirming the hazard zonation, the study area is characterized by over 80% of the events occurring in the high hazard category area.
- Probability of any sinkhole causing damage – the preliminary calculations indicate proportional increase in the *"probability of coincidence"* as well as the *"probability of damage"* with increasing diameter of a circumscribing sinkhole circle.

Data set analysis and insights suggest that the current hazard rating of the study area is *"intolerable"* and housing development is not sustainable.

Conclusion

Quantitative estimations for sinkhole events which occur in the urban environments are critical. One of the most important aspects in the hazard assessment process is data quality, and therefore, lack of data inventory, which is a crucial step in the process, makes it impossible to compile a hazard map. The greatest challenge is access to archives at relevant authorities or when accessed, available data sets are incomplete to allow for credible retrospective analysis and the quantitative estimation of the problem.

If in the future local authorities, private property developers, national agencies (housing, roads, etc.), bulk service providers and individual home/ property owners, are mandated to report all dolomite related ground instability events into a central databank, the risk assessment practitioners and engineering geologists will have a starting point when trying to assess dolomite sinkhole hazard. Therefore, implementation of appropriate risk mitigation measures, legislated basic sinkhole inspection (initial event dimensions, location, date, cause, etc.) and reporting requirements are needed.

References

Alcantara-Ayala, I. Geomorphology, natural hazards, vulnerability and prevention of natural disasters in developing countries. *Geomorphology Volume 47*. Elservier Science (2002), pp 107-124.

Buttrick, D.B.; Van Schalkwyk, A.; Kleywegt, R.J.; Watermeyer, R. Proposed method for dolomite land hazard and risk assessment in South Africa. *South African Institution of Civil Engineering Journal*. Volume 43 (2) 2001, pp 27-36, Paper 462.

Buttrick, D.B.; Trolip, N.Y.G.; Watermeyer, R.B.; Pieterse, N.D.; Gerber, A.G. A performance based approach to dolomite risk management. *Environmental Earth Sciences*. 2011 (64), pp 1127-1138.

Dippennar, M.A.; van Rooy, J.L.; Diamond, R.E. Engineering, hydrogeological and vadose zone hydrological aspects of Proterozoic dolomites (South Africa). *Journal of African Earth Sciences.* Volume 150 (2019), pp 511-521.

Jennings, J.E.; Brink, A.B.A.; Louw, A.; Gowan, G.D. Sinkholes and subsidences in the Transvaal dolomites of South Africa. *Procedures of VI th International Conference on Soil Mechanics & Foundation Engineering*, Montreal. Volume 1/11, 1965, pp 51– 54.

Jennings, J.E. Building on Dolomites in the Transvaal. *South African Institute of Civil Engineering – Commemorative Journal.* Geotechnical Division, February 1966a.

Kirsten, H.A.D.; Heath, G.J.; Venter, I.S.; Oosthuizen, A.C. The issue of personal safety on dolomite: Update of a probability-based evaluation with respect to singlestorey residential houses. *Journal of the South African Institute of Civil Engineering.* Vol 56 No. 2, August 2014, pp 78-87, Paper 719.

South African National Standards. Development of dolomite land – SANS 1936:2012 – PART 1 to 4. *Editions 1 Published by SABS Standards Division.* Pretoria 0001.

GEOMECHANICAL CHARACTERIZATION AND GEOTECHNICAL INPUTS FOR SARIÇAY DAM

GÖRKEM BAŞER[1], AYHAN KOÇBAY[2], YALÇIN ŞENTÜRK[3]

[1] State Hydraulic Works, Turkey, gorkembaser@dsi.gov.tr

[2] State Hydraulic Works, Turkey, akocbay@dsi.gov.tr

[3] State Hydraulic Works, Turkey, ysenturk@dsi.gov.tr

Introduction

In this study, the efforts made to determine the ground strength parameters of Sarıçay Dam will be explained. Sarıçay Dam (western Turkey) is a 125 m high, Roller Compacted Concrete (RCC) dam founded on Precambrian aged gneisses of the Menderes Massive, being built to meet the drinking water needs of the region. In-situ test data and rock mass classification systems were utilized to determine the strength parameters.

Methods

The variety of in-situ test methods provided important data in order to characterize Precambrian aged foundation rock, subjected to tectonic phases and various degrees of metamorphism. Engineering geology map prepared and strength parameters were evaluated via in-situ tests such as Probex Dilatometer, Goodman Jack, seismic refraction and downhole seismic. After ground stripping and removal of alluvium and highly weathered rock in the foundation, mapping and site studies carried out at dam site and it provided important data for the geomechanical modeling.

While creating the geomechanical model, laboratory and in-situ test data and observations on site were evaluated together in order to determine the shear strength and deformation modulus parameters which are the most important input parameters in the static and dynamic design of a concrete dam. The in-situ deformation moduli determined by in-situ tests using loading and unloading behaviour of rock and they evaluated together to suggest input parameters separately for each geomechanical class.

Table 1. Suggested rock mass parameters

Parameter	Right bank	Thalweg	Left bank	Conduit
Angle of internal friction, Φ (°)	38	39	33	33
Cohesion, c (MPa)	700	750	450	500
Deformation modulus (GPa)	2,2	2,5	1,7	2

Results

As a result of the findings; the stripping excavation on the left bank was deepened by approximately 30 m, and the dam face slope was changed to 1H/4V with the revised parameters. In addition, it was decided to perform consolidation grouting at 3 m intervals at a depth of 20 m due to the low strength zones encountered at shallow depths. Due to the changes in dam design and stripping excavation depth, the dam body was lengthened by 40 m and the volume of the dam body increased by 30 percent.

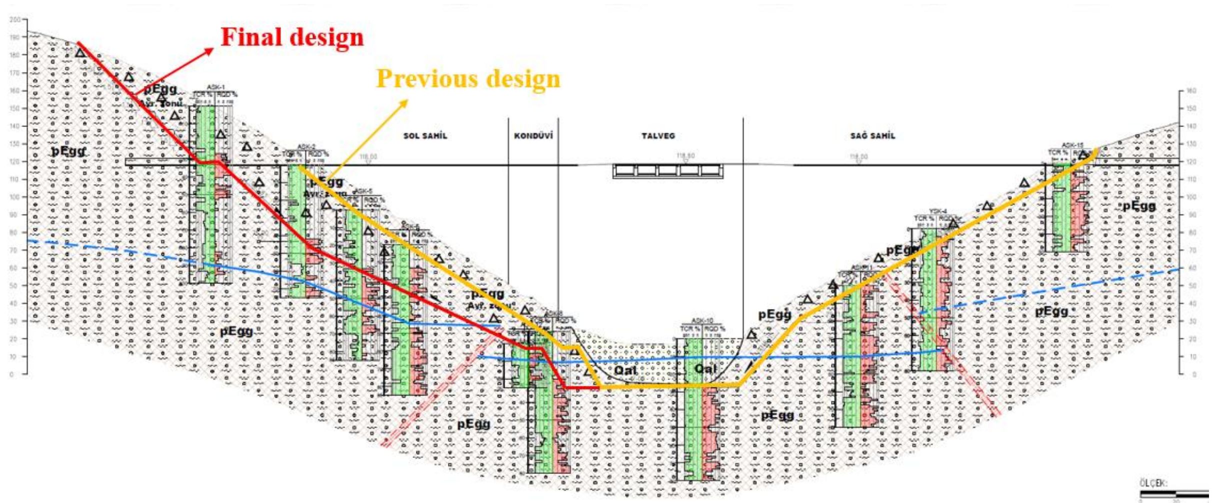

Figure 1. Stripping modification after geomechanical characterization

Conclusion

Metamorphic rocks show heterogeneous structure due to both the effect of metamorphism and intense tectonic movements. Increasing the number of in-situ experiments and the variety of methods in places with such heterogeneous mechanical properties provides important contributions to the classification of geomechanical properties.

EVALUATION OF THE STABILITY OF THE DIKE SYSTEM OF THE ŠPANIA DOLINA TAILINGS POND, SLOVAKIA

MARTIN BEDNARIK[1], RENÉ PUTIŠKA[1], BIBIANA BRIXOVÁ[1], RUDOLF TORNYAI[1], RÓBERT CSIZMADIA[2]

[1]*Comenius University Bratislava, Faculty of Natural Sciences, Department of Engineering Geology, Hydrogeology and Applied Geophysics, Slovakia; mbednarik@uniba.sk*

[2]*GEOFOS, Ltd., Žilina, Slovakia, robert.csizmadia@geofos.sk*

Introduction

In 1983, the tailings pond was in a state of emergency with water seepage and a breach in the stability of the dam. The rehabilitation of the tailings pond consisted of the reconstruction of the drainage system, the construction of an embankment weight bench made from the heap material, the filling of the created lagoon and the construction of additional monitoring probes. The Špania Dolina tailings pond was used from 1977 to 1999 to capture solid substances contained in the wastewater from the flotation treatment plant, which processed several types of raw materials. Initially, it processed copper ores, later Hg ores and finally talc-magnesite raw material. The assessment of the stability of the dam using the deformation method showed the relative strength of the tailings body, with the exception of the stability on the shear surfaces above the dark sludge. As a remedial measure, the berm was drained with a subsurface and surface drainage system and a gravity embankment was constructed. No further drainage systems were constructed until the tailings pond was closed. In 2000, the stability of the tailings dam was assessed as part of its reclamation and the condition of the tailings pond was continuously monitored. In 2021, a comprehensive assessment of the safety elements of the Špania Dolina tailings pond was required, including an assessment of the stability conditions of the dam based on variant stability calculations and the construction of a modern monitoring network (Putiška et al., 2022).

Methods

Geotechnical, engineering geological, drilling, laboratory and geophysical work was undertaken to provide a comprehensive assessment of the stability of the tailings dam system. This work included the installation of inclinometric and piezometric boreholes, dynamic penetration probes (DPP), surface geophysical measurements (electrical resistivity tomography - ERT, seismic refraction tomography - SRT, MASW, electromagnetic induction - EMI) and borehole logging. The condition of the drainage system was assessed using camera surveys and a comprehensive reconnaissance of the area surrounding the sludge pond. In order to assess the influence of the relief on water inflows into the body of the tailings pond, a map of relief slope vectors was created (Fig. 1). Above the level of the tailings pond are the steep slopes of the surrounding hills, forming a relatively large area of the imaginary micro-watershed of the tailings pond plain. On the area of the tailings pond and its surroundings, the inspection revealed several deficiencies regarding the drainage of the tailings pond area and the drainage of water from the surrounding slopes. Due to the saturation of the deposited material with water, seepage of the dam occurs at the level of the foot of the bottom berm of the tailings pond. The occurrence of leaks in the vicinity of drainage measures points to their poor efficiency and the need to dewater the tailings pond.

Results

The stability conditions of the tailings dike system were evaluated based on the q_{dyn} results from the DPP point to a state related to the saturation of the tailings pond during the period of conducting the penetration tests (April 2022). According to the defined criteria, the environment of the embankment system was divided into quasi-homogeneous layers. The first group (red colour) with a q_{dyn} value of 0 to 3 MPa represents an unstable environment, the second group (yellow colour) with a q_{dyn} value of 3 to

7 MPa represents a conditionally stable environment, the third group (green colour) with a q_{dyn} value greater than 7 MPa represents a stable environment (Fig. 2).

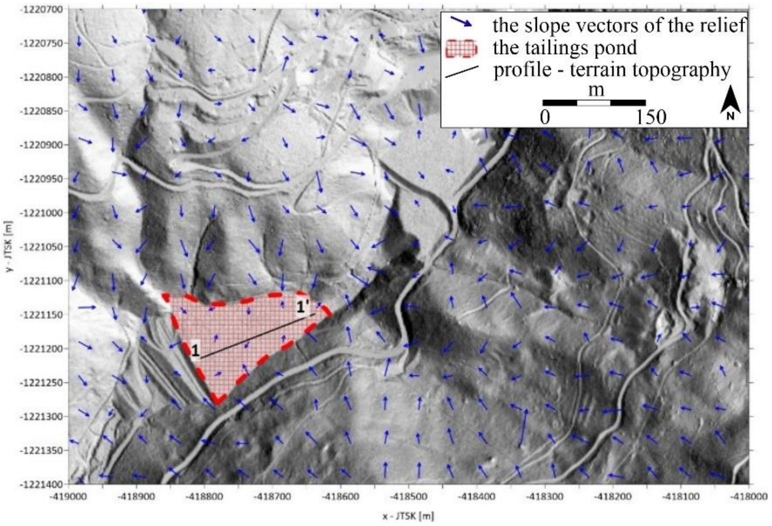

Figure 1. Map of the slope vectors of the relief

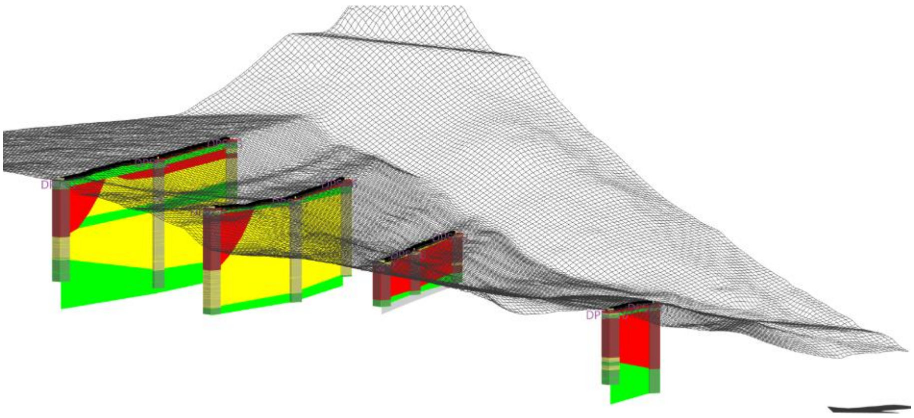

Figure 2. Visualization of continuous q_{dyn}

Conclusion

The results of the monitoring system observations and stability calculations indicate that the saturation of the tailings pond responds to seasonal variations and associated precipitation. This analysis suggests that, under the most unfavourable conditions, the tailings dam system is a system with stable conditions close to equilibrium over virtually its entire length and height. Based on a comprehensive evaluation of the safety elements of the tailings pond, a modern monitoring network has been designed and built with continuous on-line collection of information and warning conditions.

References

Putiška, R., Bednarik, M., Ciszmadia, R., Solčiansky., Jurčák, S., Dostál, I., Brixová, B. *Zhodnotenie bezpečnostných prvkov odkaliska Špania Dolina – nové a možnosti recyklácie uložených banských odpadov. Záverečná správa.* AEGEO, s.r.o., Bratislava, 2022.

Acknowledgments:

This research was partly funded by the Agency of the Ministry of Education, Science, Research and Sport of the Slovak Republic, VEGA, grant project No. 1/0182/23 "Quantification of landslide risk in urbanized areas of Slovakia threatened by the devastating effects of slope movements" and VEGA 1/0180/24 „Application and evaluation of the results of multifunctional analysis of surface seismic waves (MASW) in geological engineering and geotechnical tasks".

Investigations in Mining Projects – Innovation Challenges

MARCIO LEÃO [12], SIMMON SOUZA[1], LUIZ MOTA[1], EDUARDO MARQUES[2]

[1] *Tractebel Engineering, Brazil,* marcio.leao@tractebel.engie.com , simmon.souza@tractebel.engie.com , luiz.mota@tractebel.engie.com

[2] *Federal University of Viçosa, Brazil,* eduardo.marques@ufv.br

Introduction

Geotechnical projects in mining, compared to geotechnical projects in civil engineering, have similar characteristics of data acquisition, such as geological-geotechnical investigations, *in situ* tests, and sampling for laboratory tests. Strategic changes in mining allow basic studies (hydrological, geological, and geotechnical) to occur eventually untimely, creating obstacles to bypassing already disposed materials or constructed structures, and limiting investigation methods, especially at depth. In terms of challenges in the investigation, we can also mention the restriction of the use of pressurized water, the adoption of drilling fluids (when performing permeability studies) and knowledge of their influence on the environment, the tooling composition of the equipment used for deep geotechnical holes, the use of special samplers, the choice of appropriate samples, and the execution of *in situ* tests. Despite good engineering practices guiding procedures in widely known standards, these are not enough for obtaining this information, requiring adjustments or even modifications; however, these alternative techniques must be validated (MARQUES & LEÃO, 2023). This extend abstract discusses the operational methodology of soil infiltration tests using the wireline system as an alternative to the conventional method in deep soils in mining projects in Brazil.

Methods

The methodology was based on the authors' observations in fieldwork and kick-off meetings with drilling service companies, in addition to evaluating the procedure, as an alternative to the conventional method for evaluating the soil permeability test (MARQUES & LEÃO, 2023).

Results

Figure 1 illustrates the permeability test conducted with a non-conventional diameter (BWL). In this representation, it is possible to observe a higher probability of leakage between the outer wall of the BWL rod and the inner wall of the HQ rod. This system is seldom used in engineering projects due to the lack of studies on the application of diameter reductions of *in situ* permeability tests, raising questions about the efficacy of the test and the driving of the rods. It is worth noting that the shoe is formed by a thin cutting piece, approximately 0.8 mm thick, while the annular space between the HQ crown and the BWL is 8 mm. It is also emphasized that due to the absence of rod centralizers and calibrators, there may be non-linearity of the BWL rod, and therefore the results may present uncontrolled variables due to the variation of the perforated space. Moreover, as the hydraulic load of the drilling column increases (as a result of deeper tests), the probability of water return increases.

By physical principle, the size of the contact area is directly proportional to the resistance, meaning that the wider the tool wall, the greater the difficulty of driving the tool without causing wall collapse. In locations without prior knowledge, tests may not be conducted at the desired depth but rather at a deeper position (necessitating telescoping). In stratified materials of thin thickness, this procedure becomes more critical, making it impossible to conduct the test in the section drilled with HQ. Given the absence of technical-scientific studies on the presented methodology, it is not possible to assess the influence of subsurface variables or the procedure itself.

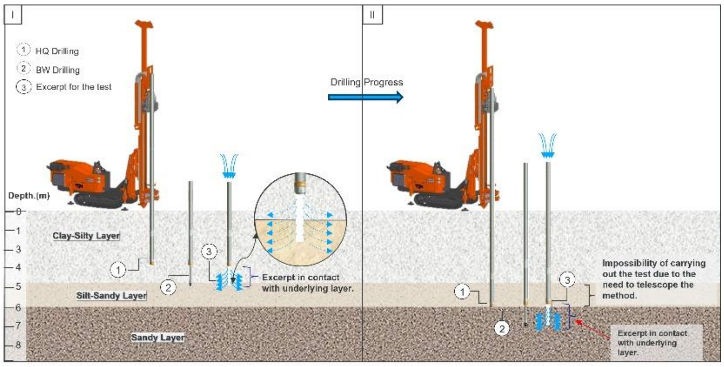

(a)

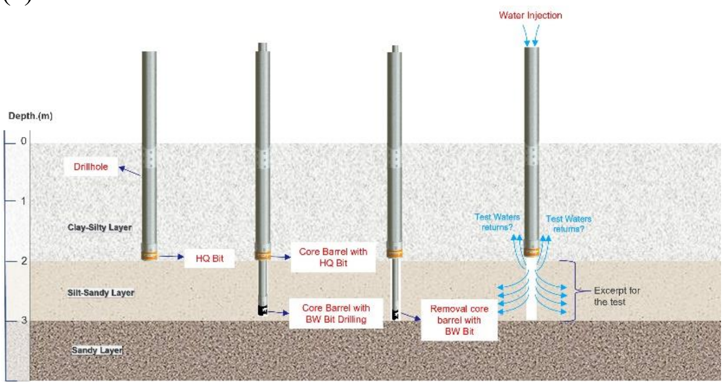

(b)

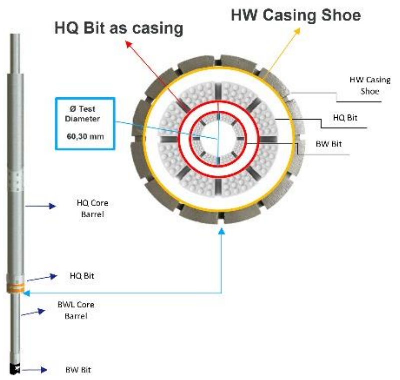

(c)

In (a), the methodology for performing the infiltration test using the wireline system:(1) Drill with the HQ rod to the desired depth. (2) Use the BWL rod to perform a telescoping operation, advancing over the underlying layer. In this way, the HQ rod would function as a casing. (3) The BWL rod is retracted to the same level as the HQ rod, thus freeing the section for the test. In (b), a detail of the procedure, and in (c), a comparison between the conventional methodology and the wireline system.

Figure 1. Execution Procedure of Soil Infiltration Test Using the Wireline System.

The evaluation of permeability values should be correlated with geological conditions (BUREAU OF RECLAMATION, 1995). It is a highly variable parameter, especially in tropical residual soils with extensive granulometry, where the finer particles are generally aggregated in their natural state. The comparison between methods and variables must have statistical support (LÓPEZ-ACOSTA et al. 2019). Ununderstood hypotheses, such as flow geometry, measurement scales, and test methodology, hinder the understanding of the results obtained by the procedure. It is important to note that the larger the volume of the tested section, the greater the influence of the massif's characteristics. This characteristic is valid for both shallow and deep tests, due to the soil's maturity.

Conclusion

For the adoption of new procedures, it is necessary for these methodologies to undergo critical evaluation to assess the influence of changing factors associated with the modification of conventional tools in different geological materials and with a higher number of tests. Therefore, research must evolve by considering the variables that influence the results.

References

López-Acosta, N.P.; Espinosa-Santiago, A.L.; Barba-Galdámez, D.F. *Characterization of soil permeability in the former Lake Texcoco, Mexico*. Open Geosciences, 2019.

Marques E.A.G; Leão, M.F. *Descomplicando a Geologia de Engenharia*. São Paulo, ABGE, 316 p., 2023 (in portuguese).

U.S. Department of the Interior, Bureau of Reclamation. *Ground Water Manual*, 690 p., 1995

DESIGN OPTIMIZATION OF PILES IN WEAK CARBONATE ROCKS - A VALUE ENGINEERING CASE STUDY OF DUBAI - UAE.

MOHAMMED MUSTHAFA KHALEEL[1], MOHAMMED JALALUDDIN AHMED[2], KURIAN JACOB[3]

[1] *Arab Centre for Engineering Studies Dubai, United Arab Emirates, k.musthafa@aces-int.com*

[2] *Arab Centre for Engineering Studies Dubai, United Arab Emirates, m.ahmed@aces-int.com*

[3] *Arab Centre for Engineering Studies Dubai, United Arab Emirates, k.jacob@aces-int.com*

Introduction

Deep foundations in weak rock formations are typically designed, with sockets in the rock mass. The design of such foundations is based on the loading magnitude, geometry, elastic properties and the side frictional resistance of the socket length. In the designs, it is a common trend to overestimate the pile capacities, which leads to needless and inefficient use of materials such as concrete and reinforcement. Most of the published correlations of fs (skin friction) to UCS (Unconfined compressive strength) are developed based on the load tests on low-capacity piles in specific geological conditions, and the UCS values which are not necessarily representative of the test depths, resulting in large variations in the calculated foundation design depths. To overcome the problem, value engineering method- Preliminary Test Pile (PTP) can be used to optimise the pile lengths, while meeting effectively the acceptable load carrying capacities.

Methodology

As per Dubai building code (DBC) 2021 requirement, for obtaining allowable working capacity of pile based on site investigation data a global safety factor of not less than 2.5 needs to be considered, however in case of verification by static load test on piles are performed then partial safety factors as per Eurocode to be applied. Accordingly, in order to estimate insitu skin friction in weak rocks, 3 high-capacity bidirectional load tests were performed. The value engineering exercise was carried out, using Eurocode approach, through back analysis of the data to optimize the design lengths of the piles. The theoretical pile capacity was estimated based on William and Pell's method (ref. 5) was found to be 8900kN for a length of 30m. It was anticipated that a minimum a reduction +20% in pile length was considered.

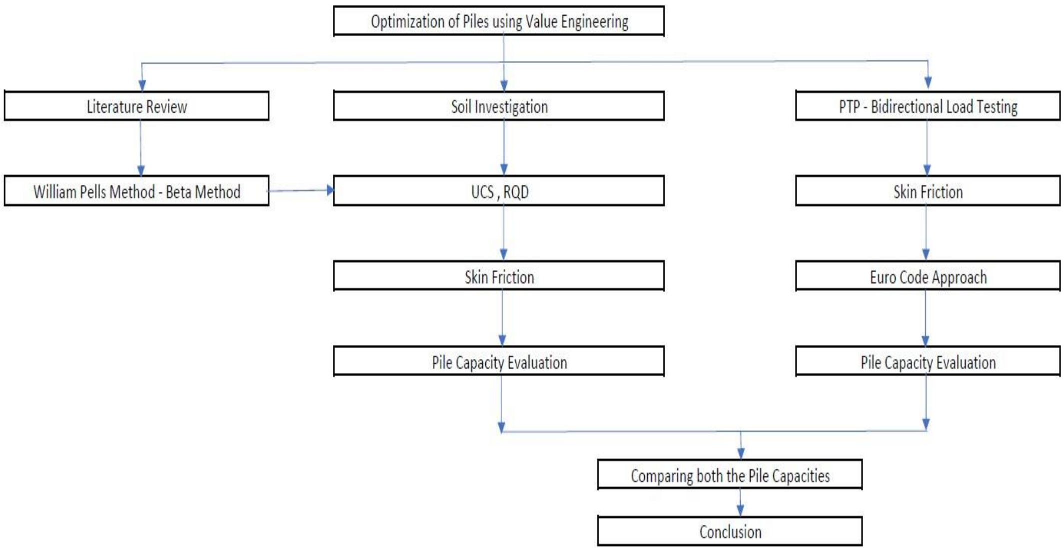

Figure 1. Methodology adopted for value engineering

Geology

The reclaimed land site in Dubai was explored with 24 boreholes depth ranges from 30 to 60m. The exploration reveals a subsurface profile with 12 to 19m thick sand, underlain by 27m of Sandstone followed by 17 m thick Conglomerate bed, and was further underlain by Siltstone up to 60m depth.

Analysis with Eurocode approach based on PTP

Eurocode 7 (ref. 1) describes three procedures for obtaining the characteristic compressive resistance Rc;k of a pile. The Rc;k is to be determined directly (i.e. not estimated) from the measured pile resistance Rc;m values (ultimate limit state resistances) by applying correlation factors $\xi 1$ and $\xi 2$ (related to number of piles tested), to the mean and minimum measured resistances according to below equation and values of $\xi 1$ and $\xi 2$.

$$R_{c;k} = Min\left\{\frac{(R_{c;m})_{mean}}{\xi_1};\frac{(R_{c;m})_{min}}{\xi_2}\right\}$$

n	1	2	3	4	≥ 5
ξ_1	1,4	1,3	1,2	1,1	1,0
ξ_2	1,4	1,2	1,05	1,0	1,0

Considering Design Approaches: DA1.C1: A1 + M1 +R1 ; A1=1.35,M1=1 and R1=1 ; DA1.C2: A2 + M1 +R4(Governing) ; A2=1,M1=1 and R4=1.4,

Design Approach-1, combination 2 is mostly governing; hence, was considered for this case study. Based on the above estimated skin frictions the allowable skin frictions were recommended. The below figure 2 shows the estimated skin frictions from PTP as well as through the theoretical estimates.

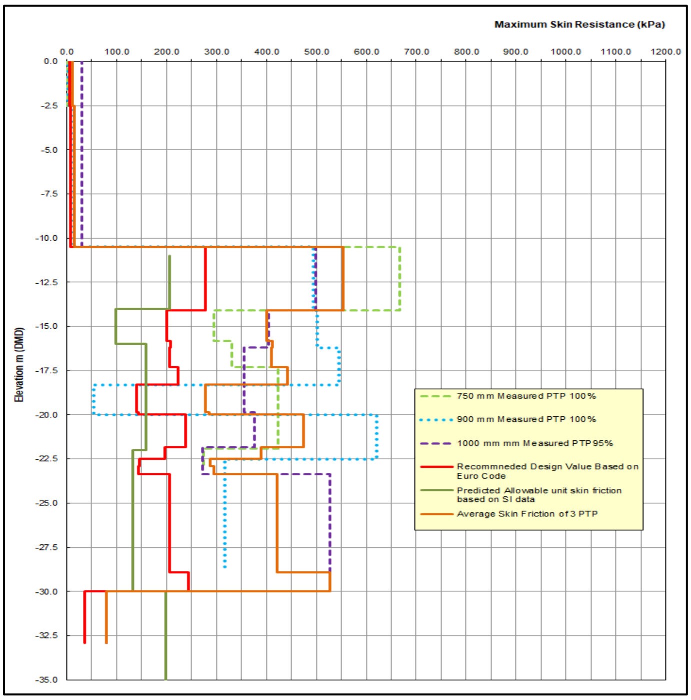

Figure 2. Graphical presentation of skin friction values from PTP

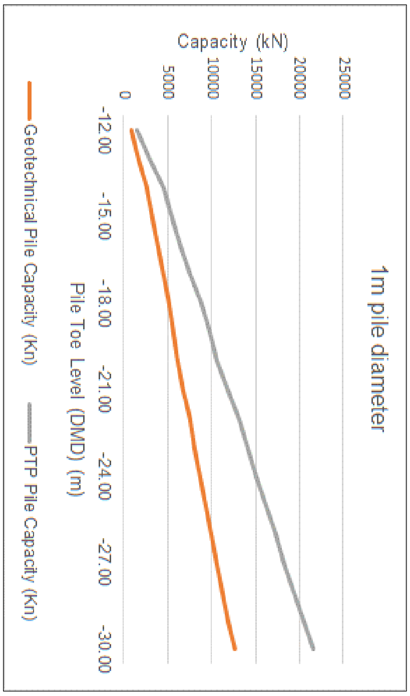

Figure 3. Pile capacities vs Toe Level

Conclusion and Recommendations:

The above value engineering method/ exercise as shown in figure 3 helped in optimising the pile lengths by over 30%. Hence, it is recommended to carry out the estimations of rock socket frictions in Intermediate Geomaterials based on the pile load tests (PTP) and optimize the design length of deep foundations. The value engineering exercise brought in substantial impact on the cost, time schedule, safety and performance of the structure.

References

1. BS EN 1997-1, *Eurocode 7, Geotechnical Design, Part 1 General Rules*, 2004
2. Deep Foundation, *A contribution for Improving current Design Practice in Dubai UAE*
3. Rowe, R.K. & Armitage, H.H., *A design method for drilled piers in soft rock.* Canadian Geotechnical Journal, Volume 24, No. 1: pp. 126-142, 1987.
4. Tomlinson, M. & Woodward, J. (5th ed.). *Pile Design and Construction Practice,* New York: Taylor & Francis, 2008.
5. William's A.F & Pells P.J.N. *Side resistance rocksocket in sandstone, mudstone and shale*. Canadian geotechnical journal, Volume 18 ,1981.

CHARACTERISATION OF EMBANKMENT ON SOFT GROUND IN THE NETHERLANDS

KEN GAVIN [1], TOM DE GAST [1], MARIO BACIC[2], SASA MEHO KOVACEVIC[2], CORMAC REALE[3]

[1] *TU Delft, The Netherlands,* k.g.gavin@tudelft.nl, t.degast@tudelft.nl

[2] *The University of Zagreb, Croatia,* mbacic@grad.hr, msk@grad.hr

[3]*The University of Bath, United Kingdom,* cr760@bath.ac.uk

Introduction

The case study area "Oostmolendijk" is located between the towns of Ridderkerk and Hendrik-Ido-Ambacht, along the river Noord in the Zuid-Holland province of the Netherlands. Oostmolendijk is a small part of the greater dyke ring IJssel-monde also known as dijkring 17. As a primary dijk, Oostmolendijk is critically important for the protection of people and infrastructure in dijkring 17. Whilst most of the dyke ring is considered stable, Oostmolendijk considered here is affected by continuous ground settlement and cracking of the road surface resulting in ongoing maintenance problems. This excessive settling and spreading relative to neighbooring dijks, leads to widespread cracking in the embankment face and the road upon it (Reale et al., 2023). The dyke has a height of approximately +4.7m NAP (Amsterdam Datum Level) with a small berm providing support at approximately +2m NAP.

The investigation consists of geophysical techniques (MASW and ERT) and geotechnical methods including additional CPTs and Borehole to obtain soil samples. An important focus of the investigation is to consider both the vertical and horizontal scales of fluctuation of the soil layers. Cone penetration tests (CPT) were carried out along the embankment at regular intervals, both on the dyke and in the field adjacent. These show a relatively uniform profile consisting of Holocene era soft soil deposits to a depth of 12 m below NAP overlying Pleistocene era coarse sands to great depth. Investigation boreholes at the site indicate that there are three different soft soil layers present within the Holocene deposits. An upper organic silty clay layer overlying a peat layer, which is in turn underlain by a lower clay. The aim of the survey was to improve geotechnical knowledge of the substratum and understand the material spatial variability, partiularly in the horizontal direction in order to identify areas of critical concern and design a suitable stabilisation method.

Methodology

The CPT programme was designed to enhance the identification of the horizontal scale of fluctuation. The CPT layout ensured multiple CPTs were positioned at each lag distance (e.g. 1m, 2m, … etc.), see Figure 1. Repeated close range measurements are crucial for accurate determination of the scale of fluctuation, as they help ensure consistent peak and trough detection. This approach maximises the efficiency of data collection while enhancing the reliability of the spatial variability analysis.

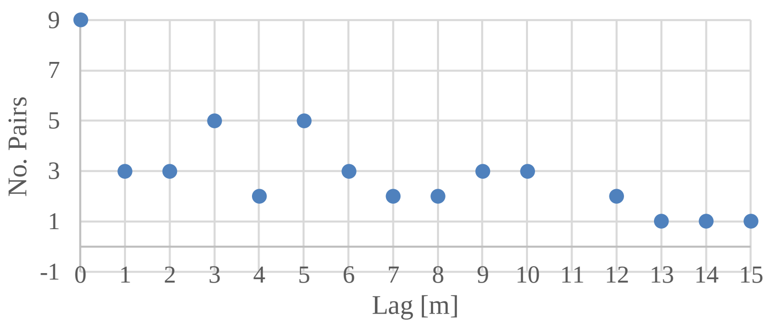

Figure 1 CPT pairs versus lag distance, ensuring repeated measurement at close lag distances.

The CPTs were broken into layers for spatial analysis before being decomposed to investigate the underlying spatial structure. A Gauss-Markov correlation function was then fitted to the underlying structure using a least squares approach (Reale et al., 2022). The results were then interpreted vertically and horizontally to determine the scales of fluctuation.

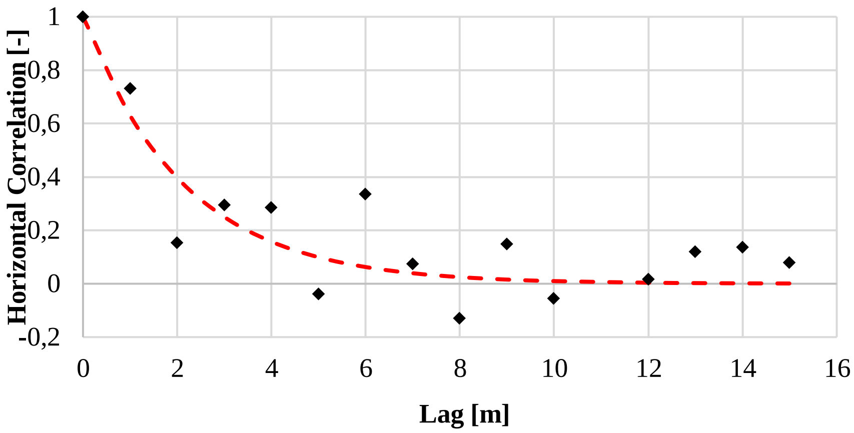

Figure 2 Horizontal correlation for the peat layer, red dashed line indicates fitted Gauess Markov model, showing a horizontal scale of fluctation of 5.14m

Results and Conclusion

Initial results at Oostmolendijk show a significant difference in the horizontal scale of fluctuation between the layers, with the deeper Pleistocene sand layers having reasonably small horizontal scales of fluctuation less than 1m. While the Holocene soft soil deposits exhibit far larger horizontal scales of fluctuation of up to 5.14m, see Figure 2. This indicates that across the linear dijk there is likely to be zones of high relative weakness in the soft clay and peat layers. Designing the CPT layout to maximise the number of CPTs at close range lag spacings enhanced data collection and ensured accurate horizontal scales of fluctuation could be obtained from all layers The next steps at the site are to interpret the laboratory testing and geophysical surveys and correlate them with the CPT results to build a full ground model to identify potential zones of weakness.

Acknowledgement

This research was funded by European Union Horizon Europe Programme, GA 101104283, CIRCUIT project (Holistic approach to foster circular and resilient transport infrastructures and support the deployment of green and innovation public procurement and innovative engineering practices.).

References

Reale, C., Kovačević, M.S., Bacic, M. and Gavin, K.G., 2022. Assessment of the spatial variability of a Croatian flood embankment using the cone penetration test. In Cone Penetration Testing 2022 (pp. 1053-1057). CRC Press.

Reale, C., Gupta, A., De Gast, T. and Gavin, K., 2023. Assessing the vulnerability of a Dutch river dyke to rising water levels. In 14th International Conference on Applications of Statistics and Probability in Civil Engineering 2023.

ABOUT GEOTECHNICAL INVESTIGATIONS OF A SALT DOME IN THE FOUNDATION GROUND OF A MOTORWAY BRIDGE

EMILIA ELENA MILUTINOVICI [1], ERBIL BALLIKAYA [2], DANIEL MIHAILESCU [3], GABRIELA DRAGOMIR [4]

[1] *AGIM, Romania*, emiliamilutinovici@gmail.com
[2] *AGIM, Romania*, erbilballikaya@gmail.com
[3] *PROSPECT TECHNICAL STUDIES, Romania*, daniel.mihailescu75@gmail.com
[4] *PROSPECT TECHNICAL STUDIES, Romania*, gabriela.dragomir@prospects.ro

Introduction

The EU's trans-European transport network policy, the TEN-T policy, aims to develop a more efficient and high-quality transport infrastructure across the EU. Romania has the privilege to develop during this period many infrastructure projects to ensure the implementation of the TEN-T framework on its territory. These projects are in different stages of implementation, from feasibility studies to design and execution. In the southern part of Transylvania, in-situ investigations were carried out for the design of a motorway sector. The section is known to be an area with a good foundation ground, comprising a covering formation made up of alternating fine or coarse stiff, uncohesive deposits, and a marly bedrock. Following the site investigations, a body of salt was identified underground that extends along the length of the highway for about 500 m. The salt body occurs at depths between 17.00 and 23.00 m, down to depths of 40.00-45.00 m. It is much thicker in its eastern part, of about 20.0 m, thinning to the west, where its thickness is reduced to 5.00 m. Salt does not appear over as a massive body and is dispersed with in the marly formation that constitutes bedrock.

Methods

The salt body is associated with other types of soils that can be constituted as difficult foundation soils. Thus, around the salt body there is a typical formation, called "salt brecia" (also described in point 8), but also "sinkhole" areas (depression, collapse or suffocation), of circular or semicircular shapes, in a depression form, sometimes as a water hole (with fresh water), surrounded by typical hydrophilic vegetation. Following the information collected from the nearest City Hall, it was confirmed that there were no salt exploitations that used water injection and saline extraction, so from this point of view, theoretically, there is no risk of the existence of caverns due to salt exploitation. However, the formation is crossed by groundwater, also in the area being historically known a well (it has not been identified at this time on the ground), from which the locals used to extract salt water for food preservation. The existence of sink-hole water accumulations in the area shows that in the past there have been collapses at the level of the salt deposit. Cracked soils appear, also called "salt brecia", associated with the salt body. Their cracking is due to the geological growth of the salt body. It can occur in the upperside or bedside area of the salt body, or can be interspersed with it, and is made up of centimetric fragments of marl or marl sites mixed with centimetric fragments of crystalline or recrystallized salt. The existence of salt bodies can also be associated with faults or anticline zones.

A number of investigations were perfomed in-situ the area.

- 20 boreholes with depth between 30.00 and 80.00 m
- in some of the boreholes, SPT test were performed
- Menard presiometer test were performed in 3 level of depth
- An exhaustive geophysical survey consisting by electric sounding and seismic refraction

Results

In general, the stratification found in geotechnical drilling is made up of covering formation and base rock. The covering formation is of Pleistocene age and is mainly made up of fine or coarse non-cohesive deposits, medium dense up to average depths of -10.00 m, which rest on thick non-cohesive deposits. At the top of them there are also clayey-dusty intercalations. The base rock, of Miocene age, is made up

of marly clays, clayey marls, marls, with some thin intercalations of sandstones or cemented sands.
At the top of the base rock was found the salt deposit, with thicknesses between 5.00-25.00 m, in the eastern part with thicknesses of 25.0 m, tapering to the west, where it reaches thicknesses of 5.0 m or even less. The salt deposit appears both as a finely disseminated salt, mixed with the mass of marly clay, especially in its edge areas, but also as a massive salt. In the western part, the salt has a migrated nature, on the layer surface, recrystallized. The depth at which the salt deposit was found is as follows:

Table 1. Salt formation limits

Borehole	Salt formation upperside depth (m)	Salt formation bedside depth (m)
F739	-	-
BH13_1	21.50	22.00
F740	20.00	20.50
BH13_2	20.00	20.50
F741	17.00	23.00
BH13_3	18.70	22.30
F742	19.50	24.00
BH13_4	24.30	26.00
F743	20.00	26.00
F744	24.00	25.00
BH13_5	25.50	41.00
BH13_5a	22.00	37.00
F745	-	-
BH13_6	24.10	38.40
F746	20.50	38.50
BH13_6a	16.90	41.00
BH13_7	16.50	40.00
BH13_7a	15.70	39.80

As a result of the geophysical investigations, the contour of the salt body was determined, the propagation speeds of the seismic waves were identified, and the values for dynamic parameters and the Poisson coefficient were established for the analyzed strata. The quality class of the soils encountered was also established, in accordance with the provisions of Eurocode 8.

Conclusion

Considering the fact that this salt body is part of the foundation ground of a future viaduct, whose project involved indirect foundation, on piles, it became extremely important to know the geometry and its properties, in order to choose a feasible foundation method.
The in-situ investigation program involved geotechnical drilling, in-situ tests (penetration and presyometric tests) and geophysical investigations. The result of the interpretations of field and laboratory investigations will lead to the choice of a design solution that will ensure the stability and integrity of the future construction.

References

ASRO. (2008, iulie). SR EN 1997-1 Eurocod 7: Proiectarea Geotehnica; Partea 1: Reguli generale. *ASRO Standard Roman*, pg. 18-19.

MDRAP. (2014). Normativ privind documentatiile geotehnice pentru constructii - NP074-2014. *Monitorul Oficial, partea I*, 1-14.

IMPORTANCE OF ENGINEERING GEOLOGICAL INVESTIGATION FOR CONSTRUCTION OF INFRASTRUCTURAL PROJECTS

MARKO COPIĆ [1]

[1] *Croatian Geological Survey, dept. of Hydrogeology and Engineering Geology, Zagreb, Croatia, mcopic@hgi-cgs.hr,*

Introduction

A project for the construction of high voltage overhead transmission lines (OHTL) in Norway started in 2016. Typical high voltage line consists of 3 main parts: foundations, steel lattice towers, and electrical conductors (wires). In this project every tower had 4 "legs", each connected to its foundation. Two general foundation types (Statnett SF 2016) were designed: 1) rock foundation with steel rebars vertically anchored into the bedrock, and 2) soil foundation with a concrete foot plate buried at designed depth (2 - 4.5 m). This work presents the events occurred during the construction of foundations for 6 towers located in an agricultural area and the conducted geological and geotechnical investigations. Construction works had to be executed when the ground was frozen to prevent damage made by vehicles. Soil excavations started in February 2017. After approx. 1.5 m of humus, a layer of light grey material appeared. Based on visual check, material was classified as silty clay with significant amount of water content, relatively soft at surface, but it didn't seem like a concern. Designed excavation depth was more than 3 m and excavator started to excavate this material. Immediately after, the material started to change its properties significantly. It became extremely soft, almost liquid, with tendency to flow, excavated pit walls were collapsing and the excavator was sinking in it, but undisturbed parts of the material were still relatively stiff. According to behaviour of this material it was assumed to be sensitive or quick clay. Construction of six foundations within the time schedule in this material was a challenge.

Methods

Geological data consisted of geological maps of bedrock (Norges geologiske undersøkelse (NGU)), description of the line route, (geological setting, definition of rock type and drillability parameters) (Statnett SF 2016), rock foundations design rules (Statnett SF 2016) and instructions for classification of the rock ground (Statnett SF 2016). Rock classification and soil type determination were conducted prior to construction. There was a concern that designed foundations were not suitable due to very poor physical-mechanical properties of the material. Differential settlements were expected and waiting for laboratory testing for calculating foundation design would take too long. Therefore, it was decided to try with in-situ experimental solutions. In situ and laboratory tests were conducted later (Table 1) at tower site where the material was so soft that calculated piled foundations had to be built.

Results

According to geological maps 1:50,000 and geological description of the line route, heterogeneous migmatitic gneisses covered with quaternary deposits (moraine, gravel, sand clay) were expected in the area. Excavation showed presence of soft and sensitive material at all 6 tower sites but with different properties.

Soft sensitive clays like quick clays are well known in Scandinavia and in some regions in Canada. The salt pore water of these marine clays has been leached out since last glaciations and left a brittle mineral structure. Norwegian quick clay has a very low permeability and hence pore water pressure becomes a crucial parameter that can affect the stability of material. Soft sensitive clays, also termed quick clays, usually exhibit sensitivity greater than 30 and have remoulded shear strength less than 0.5 kPa. Sensitivity is defined as a ratio of undisturbed undrained shear strength to the remoulded undrained shear strength of the material (Thakur et al., 2006).

Some excavation pits were performed 1 - 2 weeks earlier and thin layer of ice was formed at surface of the material. At these sites the material was not extremely soft. In more recent excavation pits, material was still very soft. Fortunately, the terrain was flat and there was no danger of landslides, so the main concern was how to build foundations within required geometric tolerances as foundations settlement

Figure 1. Two excavators spreading crushed stone into the excavation pit

was expected. Accordingly, two foundation methods were tested: 1) soil improvement by compacting crushed stone in layers and construction of foundations according to the original design. Method was chosen at tower sites excavated earlier and according to the design (four separate excavation pits for each foundation) as the material seemed relatively stiff, and 2) at later excavated tower sites, change in foundation geometry was chosen. Instead of four separate and deep foundations, one big and shallower foundation foot plate was applied, with geonet and layer of uncompacted crushed stone beneath the foundation (Figure 1). Method 1) was partially successful. Compacting crushed stone made the material softer at some spots so it wasn't compacted evenly. Most of foundations built with this method had differential settlements but inside tolerances. Foundations at one tower spot built with this method had to be demolished and rebuilt due to differential settlements caused by heavy rain during concreting. Method 2) was successful at all applied tower spots. At one tower spot material was so soft that people were sinking in it so rapidly that it wasn't possible to work in it. At this tower site foundation piles were applied. Figure 1 shows laboratory and in situ test results conducted at this tower site.

Table 1. Laboratory testing results showed changes in sensitivity with depth

Depth (m)	W (%)	Remoulded Cu (kPa)	Undisturbed Cu (kPa)	St=$\frac{Cu(undisturbed)}{Cu(remoulded)}$
3	30 - 33	7	35	5
6	35 - 41	~ 0.5	8-9	16 - 19
9	35 - 37	<=0.5	13-23	25 - 40

Conclusion

It is not a rare case in OHTL industry that economic feasibility of geotechnical or engineering geological investigations are questioned due to their high costs (a lot of tower spots, difficult terrain, environmental restrictions etc). This case presents one of many possible consequences of unexpected and rare material occurrence in construction projects and emphasizes importance of detailed preliminary investigations. Fortunately, in this case the consequences were only of financial nature. Inclined terrain, higher air temperatures or lack of good planning and cooperation would probably endanger the whole project. Multidisciplinary investigations, optimised for specific project, should be part of planning process for important infrastructural projects. Engineering geological and geotechnical investigations shouldn't be considered as an expense but rather as an investment in safer construction.

References

Statnett SF *09-06-01 - AC Suspension Tower Foundation Rock %96 Tender drawing*. Statnett internal document, 2016.

Statnett SF *09-06-02 - AC Suspension Tower Foundation Soil %96 Tender drawing.* Statnett internal document, 2016.

Norges geologiske undersøkelse (NGU) (Geologiske kart). Available online: https://www.ngu.no/geologiske-kart

Statnett SF *08-01-02 - Exh E -TN Geological description 420 kV Namsos-Hofstad-Afjord.* Statnett internal document, 2016.

Statnett SF *08-03-01 Anchorage of Tower Foundations in Rock - Classification of Rock Ground_SDOK-82-14_R2.* Statnett internal document, 2016.

Statnett SF *08-03-02 Anchorage of Tower Foundations in Rock - Design Rules_SDOK-82-3_R2*. Statnett internal document, 2016.

Thakur, V., Grimstad, G., Nordal, S. *Instability in Soft Sensitive Clays,* 2006 ECI Conference on Geohazards, Lillehammer, Norway

DETECTION OF FRACTURED ZONES AND CAVERNS IN KARST USING GEOPHYSICAL METHODS AT THE LOCATION OF VIZINADA IN ISTRIA

BOŽO PADOVAN [1], VALENTINO MEJRUŠIĆ [1], MARKO MARIČIĆ [1], JOSIP MIKŠIĆ [1]

[1] *Terra Compacta d.o.o., Croatia,* bpadovan@terra-compacta.hr

[1] *Terra Compacta d.o.o., Croatia,* vmejrusic@terra-compacta.hr

[1] *Terra Compacta d.o.o., Croatia,* mmaricic@terra-compacta.hr

[1] *Terra Compacta d.o.o., Croatia,* jmiksic@terra-compacta.hr

Introduction

Geotechnical designing in Karst is often challenging because of many unknown parameters related to materials, composition and current condition of field of research. To get comprehensive picture of underground, geophysical methods presents fast and reliable solution to identify important features of underground that are later used during geotechnical designing (Yilmaz, 2015). Construction of luxurious mansion is planned in village Žudetići, municipality of Vižinada. Location of the construction site is at the edge of Pazin flysch basin where Eocene flysch is in contact with Cretaceous limestone.

Methods

During field prospecting, indications of fractured and hollow zones have been observed. In that zones during rainy periods a flow of water can be heard. This flow of water is unlike characteristic underground water flows in karst areas and instead it is represented as water pockets that sporadically move through smaller fractures and possibly small caves. Local residents describe sound of flow as “crunching” or “gurgling”.

Figure 1. Distribution of geophysical profiles.

Geophysical profiles were set along main axes of the building, perpendicular to flysch and limestone contact and along all locations with presumed fractures and caves. Geophysical methods included seismic refraction tomography and geoelectric tomography. Combination of such methods provides key parameters needed to differentiate materials and to detect fractured zones with positions of main fractures and caverns (Gebrande & Miller, 1985.) (Gibson, Odegard, & Sutton, 1979).

Results

Boundary between flysch and limestone as well as their volume and thickness were determined through electrical resistance propagation. By observing only electrical resistance propagation it is not possible to unequivocally detect fractured zones. Elastic P-waves propagation in seismic tomography confirmed forementioned boundary and showed many zones with inversion of velocity of seismic waves. Inversion in elastic P-waves velocities, which is gained by seismic inversion modelling, is significant indicator of fractured zones and caverns underground. During initial phase of construction, zones with inverted seismic velocities and increases in electrical resistivities have been confirmed as fractured zones with significant fractures and caverns.

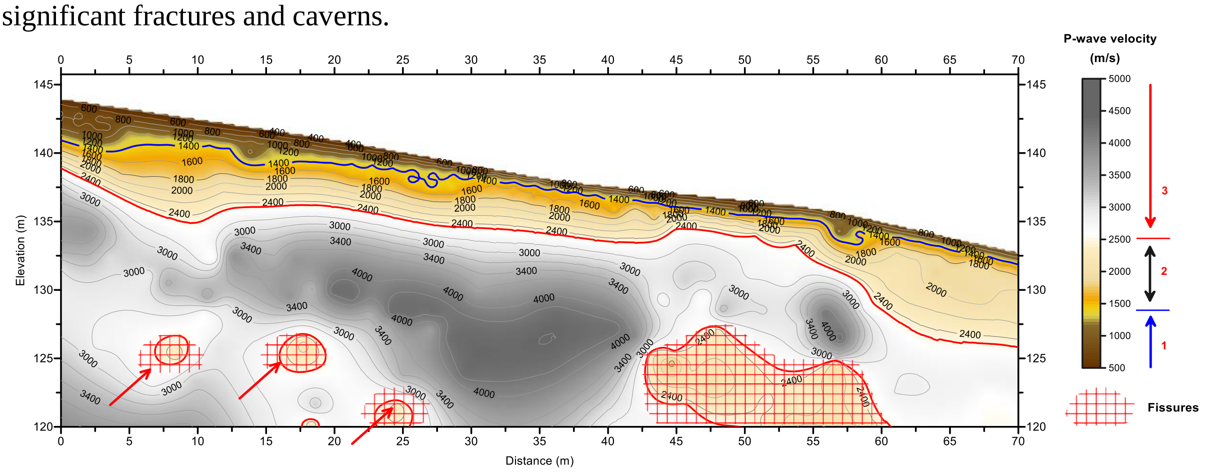

Figure 2. Seismic refraction profile.

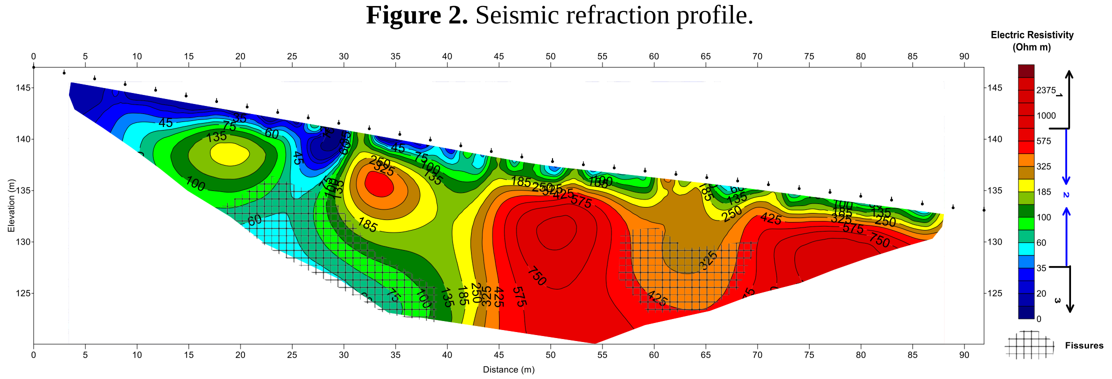

Figure 3. Electric tomography profile.

Conclusion

In order to establish as reliably as possible the existence of geological phenomena such as caverns, cavities, fractured zones, cracks, contacts between different lithological members, it is necessary to avoid the ambiguity of geophysical methods (Yilmaz, 2015). Geoelectrical tomography can distinguish between materials if they have different electrical conductivity (Loke & Dahlin, 2002), but the results can easily be affected by a number of factors such as, for example, a change in the water level (or the absence of water) underground. On the other hand, using refraction tomography, it is often impossible to distinguish between materials (Gardner, Gardner, & Gregory, 1974) due to their similar velocities (ie, compacted marl and weathered limestone), even if they have significantly different electrical conductivities. Therefore, the combination of seismic refraction tomography and geoelectric tomography increases the reliability of distinguishing materials and successfully determining phenomena such as fracture zones and caverns.

References

Gardner, G. H., Gardner, L. W., & Gregory, A. R. (1974, December). *Formation velocity and density - the diagnostic basics for stratigraphic traps*. Geophysics, 39(6), 770 - 780.

Gebrande, H., & Miller, H. (1985.). *Refraktionsseismik*. In F. Bender (Ed.), Angewandte Geowissenschaften II (pp. 226 - 260). Stuttgart.

Gibson, B. S., Odegard, M. E., & Sutton, G. H. (1979). *Nonlinear least-squares inversion of traveltime data for a linear velocity-depth relationship*. Geophysics, 44, 185-194.

Loke, M. H. (2011). *Electrical resistivity surveys and data interpretation*. In Encyclopedia of Solid Earth Geophysics (pp. 276-283).

Yilmaz, O. (2015). *Engineering Seismology with Applications to Geotechnical Engineering. Society of Exploration Geophysicists*.

SINKHOLE HAVOC TO A STATE OF DISASTER: CASE STUDY INTO A RESETTLEMENT PLAN FOR KHUTSONG NORTH COMMUNITY, GAUTENG PROVINCE – SOUTH AFRICA

BONGANI MSANE [1], SIFISO NGUBELANGA [2],

[1] *Infrastructure and Land Use, Council for Geoscience, South Africa, E-mail: bmsane@geoscience.org.za*

[2] *Infrastructure and Land Use, Council for Geoscience, South Africa, E-mail: sngubelanga@geoscience.org.za*

Introduction

Karst-related sinkholes and subsidences occur on areas underlain by Chuniespoort Group dolomite bedrock in the Gauteng Province, South Africa. Although dolomite land occurs across five of the nine South African provinces, the sinkhole problem has considerably been more severe in Gauteng than in other provinces (Constantinou and van Rooy, 2019).

Khutsong township was established in the late 1950s, as a result of the gold mining history has been a source of migrant labour for areas around South Africa and neighbouring countries, such as Mozambique, Swaziland, etc (Kirshner, 2012, *in* Tune, 2016). At the time of establishment, no geological surveys were conducted to determine the suitability of the area for urban development.

Despite the ever-increasing ground instabilities in the region, Khutsong contunued to develop until 1980 when a private firm was comissioned to conduct a first geotechnical study. From this date until at least the year-2013, several dolomite stability surveys have been conducted by various engineering geological firms and a Dolomite Risk Management Plan (DRMP) was compiled in 2004 (HDA, 2020). Inspite of these intervesions and the formation of disaster management team of the Westrand District Municipality by the then newly established Merafong City Local Municipality (MCLM), new sinkhole events continued to cause havoc across Khutsong and even in areas previously classified as safe. From 2016 to date, the situation has drastically deteriorated resulting in several house being demolished, roads closed, and the wet services network destroyed creating a local state of emergency. As a result of the intolerable rate of new sinkholes and in line with the Disaster Management Act, 57 of 2002 (DMA), a State of Local Disaster was declared on Khutsong North during November 2016.

The dolomite risk assessment study is aimed at gathering data relevant to re-assess the current situation and provide details on any additional areas for inclusion into the Khutsong North Re-settlement Plan.

Methods

The ultimate objective of the project is to align the existing development with the technical requirements as stipulated in South African National Standard (SANS) 1936:2012 for development on dolomite land and the National Home Builders Registration Council (NHBRC) 2015 Manual. Data and information were collated from a few sources for review: MCLM, ENGEODE Database of the Council for Geoscience (CGS), including site visits and stakeholder engagement meetings. Reference was also made to various published sources (maps) and previous media reports addressing the issue of dolomite risk.

Using the available reports, percussion boreholes and ground instability events occurring within the area of Khutsong North Extensions (Khutsong Proper & Extension 1 – 6), the stability of the area was re-assessed in terms of the current Method of Scenario Supposition – statistical occurrence of eight inherent hazard classes as described in SANS 1936-2:2012.

Results

The available record of ground instability events combined with geological maps, geotechnical and geohydrological data was used to assist the MCLM to outline the necessary measures and implement the Khutsong North Re-settlement Plan. The current dolomite stability risk assessment broadly subdivided the study area into two composite inherent hazard class (IHC) zones, namely: Zone 1: IHC 3 - 4//1 and Zone 2: IHC 5 – 8//1. This zonation largely reflects medium to high susceptibility of medium to very large size events with respect to ingress of water, and a low susceptibility of all-size events with respect to groundwater level drawdown. Based on the current study, the existing resettlement plan was revised, and new priority area were added to make a total of nine (9) priority areas, Figure 1.

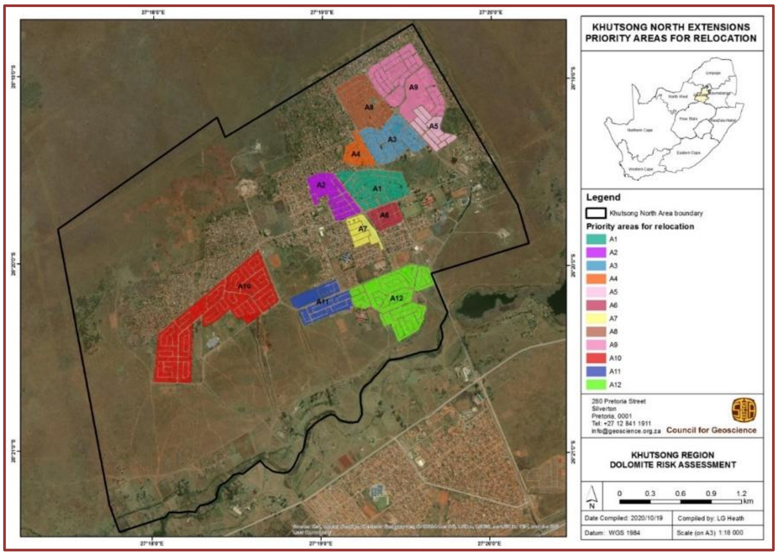

Figure 1. Priority areas identified for re-settlement, (CGS Report, 2020)

Conclusion

The regional dolomite risk assessment on Khutsong North Extensions confirmed that the area is predominantly characterised by high hazard (IHC 5 – 8), i.e. over 58% of the boreholes reveal these conditions. Furthermore, the available ground instability events (sinkholes & subsidences) recorded reveal an area dominated by larger (5-15m) to very-large size events (>15m). Most of these events are directly attributed to poor stormwater management and leaking water-bearing infrastructure. The situation has led to the demolition of many houses, closure of roads and collapse of the wet services systems, and has necessitated the consideration of an expensive re-settlement option.

In conclusion, the area is deemed generally unsuitable for residential development and at least, the upgrade of the wet services infrastructure must be implemented in the non-priority areas.

References

Buttrick, D B, Van Schalkwyk, A, Kleywegt, R J & Watermeyer, R B. Proposed method for dolomite land hazard and risk assessment in South Africa. Journal of the South African Institution of Civil Engineering, 2001, 43(2): 27–36.

Constantinou, S., Van Rooy, J.L. Sinkhole and subsidence size distribution across dolomitic land in Gauteng. SAICE Journal. 2019, Paper 1373.

Council for Geoscience. Phase A – Dolomite Stability Risk Assessment of Khutsong Proper & Khutsong North Extension 1 – 6. 2020, Report number: 2020-0129.

National Home Builders Registration Council. Home Building Manual and Guide. 2015, NHBRC Communications, Sunninghill, Johannesburg.

Tune, L. The Dynamics of Mining Towns: The Case of Khutsong Township, Carletonville. Master Thesis, University Of The Witwatersrand, Johanneburg, South Africa, 2016.

The Housing Development Agency (HDA). Review and finalisation of Programme Implementation Plan: Khutsong Sinkhole Intervention 2020, RFP/JHB/2020/011.

South African National Standard. Development of dolomite land – SANS 1936 – Parts 1-5. 2012, SABS Standards Division, Pretoria 0001.

DEM SUPER-RESOLUTION FOR PHOTOVOLTAIC SITE SUITABILITY ASSESSMENT

JIYOON KU [1], HYEONG-DONG PARK [2, 3]

[1] *Department of Energy Systems Engineering, Seoul National University, Korea, rnldbs9808@snu.ac.kr*

[2] *Department of Energy Resources Engineering, Seoul National University, Korea, hpark@snu.ac.kr*

[3] *Research Institute of Energy Systems, Seoul National University, Korea, hpark@snu.ac.kr*

Introduction

To ensure a sustainable economic return over a 20-year period, the deployment of photovoltaic (PV) installations necessitates the critical consideration of solar irradiance and site suitability. Developing solar power on unstable sites can lead to significant damage from landslides, making it essential to assess ground stability in advance. A Digital Elevation Model (DEM) serves as a crucial tool in this assessment, representing terrain surfaces through elevation data contained in each pixel. Topographic analysis using DEMs provides critical site parameters such as slope gradients and hydrological systems, essential for selecting stable sites for solar installations. High-resolution (HR) DEMs, offering more detailed analyses, are preferable but may be difficult to acquire or limited in area and scope. Evaluating the accuracy and cost-effectiveness of HR data is necessary. This study aims to compare how three critical geological parameters for photovoltaic site suitability—slope, aspect, and distance from streams—change with different DEM resolutions and how these changes affect the identification of suitable areas for PV installations. Should significant disparities between low and high-resolution DEM data emerge, future research could utilise super-resolution techniques to synthesise HR data from existing lower-resolution (LR) datasets. This study serves as a preliminary study, analysing existing DEMs of varying resolutions.

Methods

This study evaluates the impact of DEM resolution on the suitability of sites for PV installations, focusing on three distinct geographic regions in South Korea: flatlands, mountains, and mixed terrain, each spanning 2000 km². Two types of DEMs are utilised: a low-resolution DEM with a spatial resolution of 30 m (ASTER, 2023) and a high-resolution DEM with 12.5 m (ASF, 2024). The study concentrates on 3 critical topographic factors that significantly affect the viability of PV installations: slope, aspect, and distance from streams. Land stability increases with a slope inclination angle of less than 10° (Nebey et al., 2020). Unstable slope affects both the construction feasibility and risk of land movement. Solar panels in the northern hemisphere generate optimal energy on south-facing slopes (157.5°–202.5°), and sites more than 1 km from streams are preferred to mitigate flooding risks (Nebey et al., 2020). Using ArcGIS, a Geographic Information Systems (GIS) platform, three topographic factors were extracted from both the LR and HR DEMs. A detailed comparison was then conducted to evaluate how DEM resolution influences the assessment of each parameter and the sensitivity of site suitability assessments.

Results

Across all topographic factors and regions, HR DEM showed a decreased area suitable for PV installations (Table 1). For slope, HR DEMs have steeper slopes than LR DEMs, resulting in a smaller area suitable for PV installations, particularly in mountainous regions with the greatest difference in suitability. Aspect exhibited the least change between LR and HR data, implying that it is less sensitive to resolution. However, HR DEMs detected significantly more streams in all regions, reducing suitable areas due to the 1 km safety buffer requirement. Figure 1 shows that LR detects main streams (primary and secondary) comparable to HR, but has limitations in detecting detailed tributaries. The Flatlands area revealed the greatest difference, with 243 more streams identified via HR data, greatly limiting suitable sites.

Table 1. Suitable areas for PV installations based on topographic factors using LR and HR DEMs in flatlands, mountains, and mixed terrain.

Criteria	Flatlands (km²)		Mountains (km²)		Mixed terrain (km²)	
	LR	HR	LR	HR	LR	HR
Slope (under 10°)	1631.15	1564.56	221.52	195.15	773.3	744.94
Azimuth (south facing)	249.21	223.56	249.41	249.16	252.7	235.59
Distance from streams (> 1 km)	1568.32	1067.19	1616.06	1145.67	1636.72	1169.66
Combined	155.83	15.3	18.12	1.55	66.2	5.84

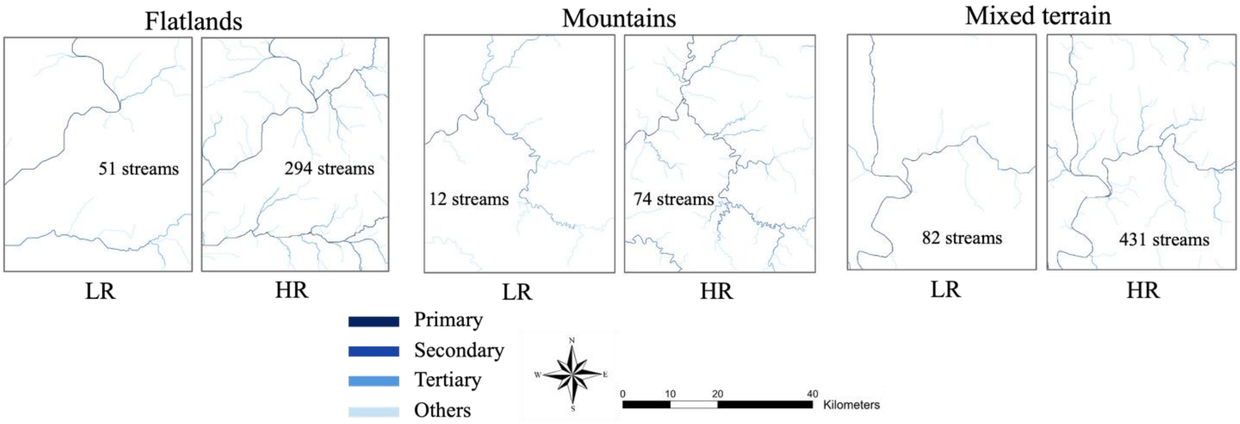

Figure 1. Stream networks identified using LR and HR DEMs in flatlands, mountains, and mixed terrain.

Conclusion

This study assessed the impact of LR and HR Digital DEMs on the identification of suitable sites for PV installations. HR DEMs identified 73 km² less suitable sites across all terrains, a 3.6% difference over the total area (2000 km²). This discrepancy arises from HR DEMs' superior ability to delineate stream networks, highlighting significant advantages of fine-resolution data, particularly in identifying areas less susceptible to flooding. Consequently, HR DEMs provide a more detailed assessment, enabling more accurate and sustainable site selection for solar installations. The findings emphasise the benefits of HR data for terrain analysis, recommending the use of existing high-quality resolution data where available or generating such data through super-resolution techniques in future research. This contributes to the strategic planning and optimisation of solar energy projects, emphasising environmental considerations and long-term sustainability.

Acknowledgement

This study was supported by Energy & Mineral Resources Development Association of Korea (EMRD) grant funded by the Korea government (MOTIE) (2021060003, Training Program for Specialists in Smart Mining).

References

ASF (Alaska Satellite Facility). available online: https://asf.alaska.edu/datasets/daac/alos-palsar-radiometric-terrain-correction/ (accessed on 11 March 2024).

ASTER GDEM 003 (Advanced Spaceborne Thermal Emission and Reflection Radiometer Global Digital Elevation Model Version 3). available online: https://asterweb.jpl.nasa.gov/gdem.asp (accessed on 7 May 2023).

Nebey, A. H.; Taye, B. Z.; Workineh, T. G. Site suitability analysis of solar PV power generation in South Gondar, Amhara Region. Journal of Energy, 2020, 1, 3519257.

ASSESSING MECHANICAL PROPERTIES OF QUARTZITIC MATERIALS AND SHEAR BEHAVIOR OF QUARTZITIC JOINTS WITH REFERENCE TO THEIR WEATHERING GRADES

ARINDAM BASU [1]

[1] *Indian Institute of Technology Kharagpur, India, abasu@gg.iitkgp.ac.in*

Introduction

The ongoing process of weathering in nature produces progressive but intricate changes in rock microstructure. The common 6-fold weathering classification scheme for uniform materials proposed by ANON (1995) is applicable for categorizing weathering grades of most polymineralic rocks. However, capturing the intricate gradational change of quartzite in response to weathering is a challenging task as quartz, the most resistant mineral to weathering, is the chief mineral constituent of quartzite. Subsequently, assessing mechanical properties of quartzitic materials with reference to weathering grades becomes difficult in an engineering environment encountering weathered profiles.

It is likely that the degree of weathering of the joint surface materials would influence the shear behavior of quartzitic joints. However, quantitative assessment of shear behavior of quartzitic joints with reference to weathering grades does not seem to have gained much attention.

This extended abstract first presents the author’s experience in categorizing weathering grades of quartzitic materials from the Chaibasa Formation (India) and evaluating their mechanical properties with reference to the categorized grades. Subsequently, the shear behavior of quartzitic joints with regard to the degree of weathering of joint surface materials, which has got tremendous implications to shallow-depth rockslides in quartzitic terrains of tropical/sub-tropical regions, is also evaluated.

Methods

Quartzitic rock materials from the Chaibasa Formation (India) were investigated by the author and his co-workers (Basu et al., 2011; 2012). An attempt was made to categorize weathering grades of these materials using the 6-fold weathering classification scheme (ANON, 1995). In order to capture the gradational variations of the quatzitic materials, observations pertaining to discoloration/staining, grain luster, intactness of grain boundaries, relative strength and slaking were utilized to discriminate weathering-induced gradational changes of the quartzite materials. It is to note that quartzite dominantly consists of quartz grains which hardly show any discoloration and the weathered appearance of the quartzitic rocks is attributed mainly to the alteration of biotite and other iron bearing minerals that are present in a small proportion (< 5% of the rock volume). Such macroscopic categorization of weathering grades was also substantiated by microstructural study as well as by rock index tests (e.g. rebound hammer test). Uniaxial compression and Brazilian tensile tests were performed on the drilled core specimens of the quartzite.

Only a handful of studies explored the influence of weathering on the shear behavior of rock joints. With regard to quartzitic joints, this issue did not seem to have been explored. The author along with his co-workers (Ram and Basu, 2019) investigated shear behavior of unfilled-planar qurtzitic joints with reference to weathering grades of joint surfaces. The weathering grades were determined exactly in compliance with the method demonstrated by (Basu et al., 2011; 2012). Multistage CNL (constant normal load) direct shear tests were performed at three different consecutively increasing normal stresses within a range of 0.22–0.70 MPa under dry condition. Since quartzite is virtually a monomineralic rock and joints with different weathering grades but with comparable joint roughness coefficient were selected for the study, the shear behavior observed in the laboratory were likely to be a direct function of weathering grade of the joint surfaces.

Results

Uniaxial compressive strength, Young's modulus and Brazilian tensile strength of the quartzitic materials were determined in the laboratory. The ranges of these values with reference to weathering grades are presented in Table 1 which broadly demonstrates an adverse effect of weathering on the mechanical behaviors. Table 1 also shows some overlap of these ranges particularly in adjacent grades.

Table 1. Mechanical properties of quartzitic materials with reference to weathering grades (from Basu et al., 2011; 2012)

Weathering grade	Uniaxial compressive strength (MPa)	Young's modulus (GPa)	Brazilian tensile strength (MPa)
I	-205.76-	-45.56-	11.35-8.99
II	114.75-51.71	15.88-6.07	8.50-2.54
III	80.00-42.46	5.22-3.45	4.79-1.87
IV	-42.44-	-1.08-	2.29-1.65

Representative shear stress-shear displacement plots of the quartzitic joints are shown in Figure 1. It should be noted that finding fresh rocks at the ground surface is unusual as reported by previous researchers. The omission/absence of Grade I joint surface in Figure 1 is attributed to the unavailability of those rocks on the investigated outcrops. A clear adverse effect of degree of weathering on the shear behavior of joints becomes apparent (Figure 1). The strength of the joint surface materials which is a function of weathering grade plays a key role in controlling the shear behavior of the joints with minimal asperities. The nature of the shear behavioural patterns of Grade II and Grade III joints are, however, similar whereas Grade IV joint shows a completely different shear stress-shear displacement pattern (Figure 1). It was not possible to carry out multistage CNL direct shear tests on Grade IV joint surfaces as the test specimens got broken after the first phase of shearing (Figure 1). Another interesting feature Figure 1 depicts is that the difference of peak strength between two dissimilar grades is maximum at the highest normal stress. This can be attributed to the crushing of asperities which is more likely to happen at relatively higher normal stresses in case of higher weathering grade. From the peak shear strength vs. normal stress plots, the peak friction angle could be determined. The ranges of peak friction angle for Grade II and Grade III joints were found to be 38°–40° and 31°–35°, respectively.

Conclusions

- The conventional 6-fold weathering classification for uniform materials is capable of capturing gradational weathering induced changes of quartzitic materials.
- As weathering intensifies, deterioration of mechanical properties of quartzite becomes apparent. The ranges of mechanical properties of quartzitic materials, however, do depict some overlaps particularly in adjacent grades.
- As weathering of quartzitic joints intensifies, both peak shear strength and peak friction angle get reduced.
- At higher normal stresses, the adverse effect of joint surface weathering on the peak shear strength becomes more prominent than at lower normal stresses.

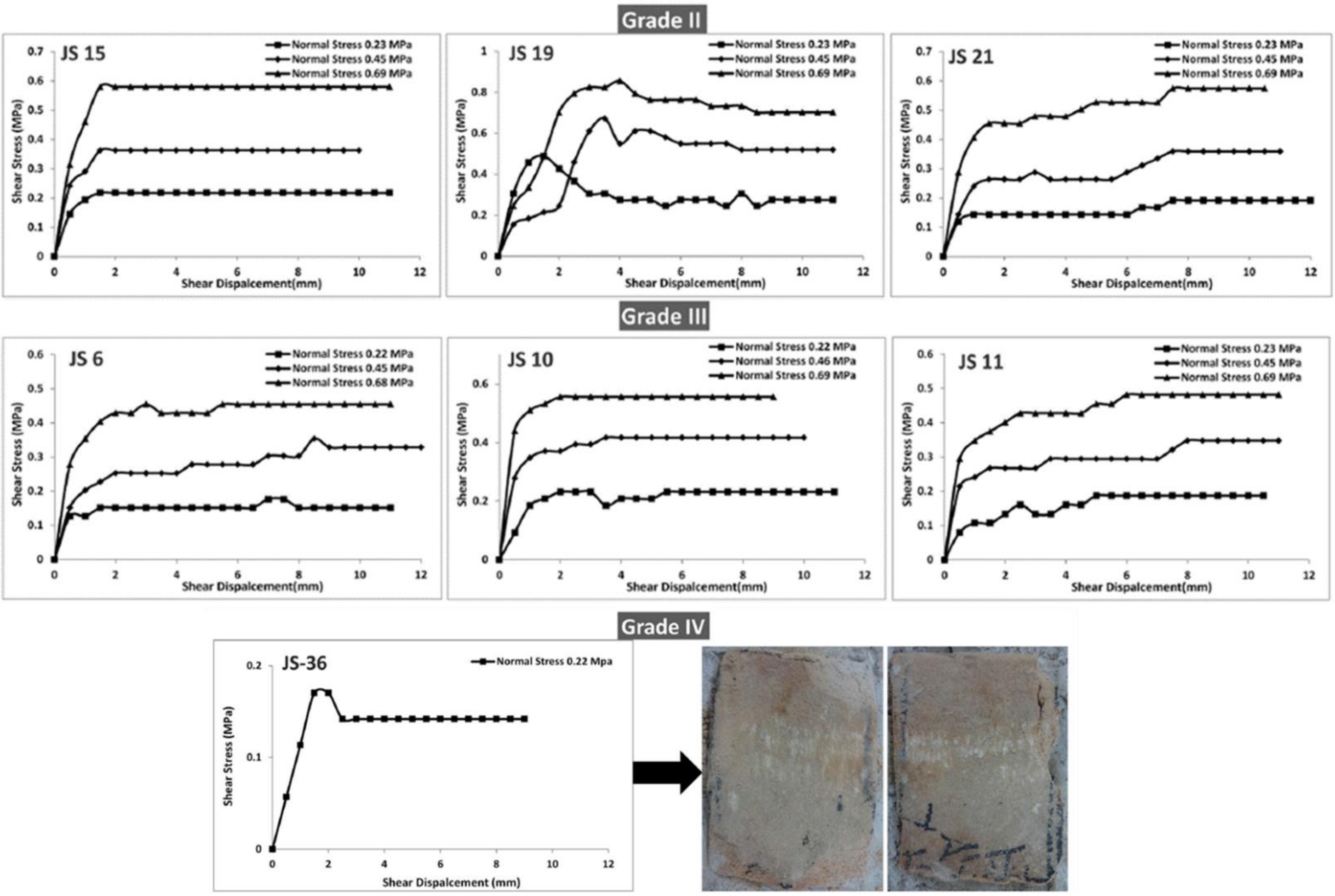

Figure 1. Representative shear stress-shear displacement plots with reference to weathering grades of quartzitic joints (from Ram and Basu, 2019)

References

ANON. The description and classification of weathered rocks for engineering purposes: Geological Society Engineering Group Working Party Report. *Quarterly Journal of Engineering Geology and Hydrogeology.* 1995, 28, 207–242.

Basu, A.; Ghosh, N.; Das, M. Weathering grade categorization and subsequent evaluation of compressive and tensile strengths of quartzite. *Journal of Engineering Geology.* 2011, XXXVII, 1–4.

Basu, A.; Ghosh, N.; Das, M. Categorizing weathering grades of quartzitic materials and assessing Brazilian tensile strength with reference to assigned grades. *International Journal of Rock Mechanics & Mining Sciences.* 2012, 49, 148–155.

Ram, B. K.; Basu, A. Shear behavior of unfilled-planar quartzitic rock joints with reference to weathering grade of joint surfaces. *Rock Mechanics and Rock Engineering.* 2019, 52, 4113–4121.

IDENTIFICATION OF GOAF AREAS AND DEFORMATION CHARACTERISTICS IN ORDOS

CHEN CAO [1], QING WANG [1], JIANPING CHEN [1], ZONGZHENG LI [1], QINGKUN YANG [1]， LIANJING ZHENG [1]

[1] *Jilin University, China, ccao@jlu.edu.cn*

Introduction

Ordos City is a significant coal production base in China, with frequent mining activities that have led to the formation of numerous goaf areas.By analyzing the deformation rate values and distribution characteristics from SBAS-InSAR results, the range of subsidence areas caused by coal mining in Ordos City can be identified. The deformation characteristics of these subsidence areas are further examined by focusing on typical subsidence zones based on their deformation rates.

Methods

In this research, SBAS-InSAR technology is employed to monitor surface deformation in the coal mines of Ordos City and obtain detailed deformation information for the study area. The deformation rate is then estimated using the singular value decomposition method, allowing for the characterization of the temporal variation in the study area.

Results

A total of 142 coal mine goaf subsidence areas were identified within the study area, covering a total of 833.83 km², with a maximum deformation of -778.362 mm.

The subsidence rate in these areas is negative, exhibiting a pattern of multi-layered circular nesting. According to the timing analysis results, subsidence in the goaf areas occurs continuously.The subsidence rate is significantly influenced by mining activities, leading to a sharp increase in settlement rates.

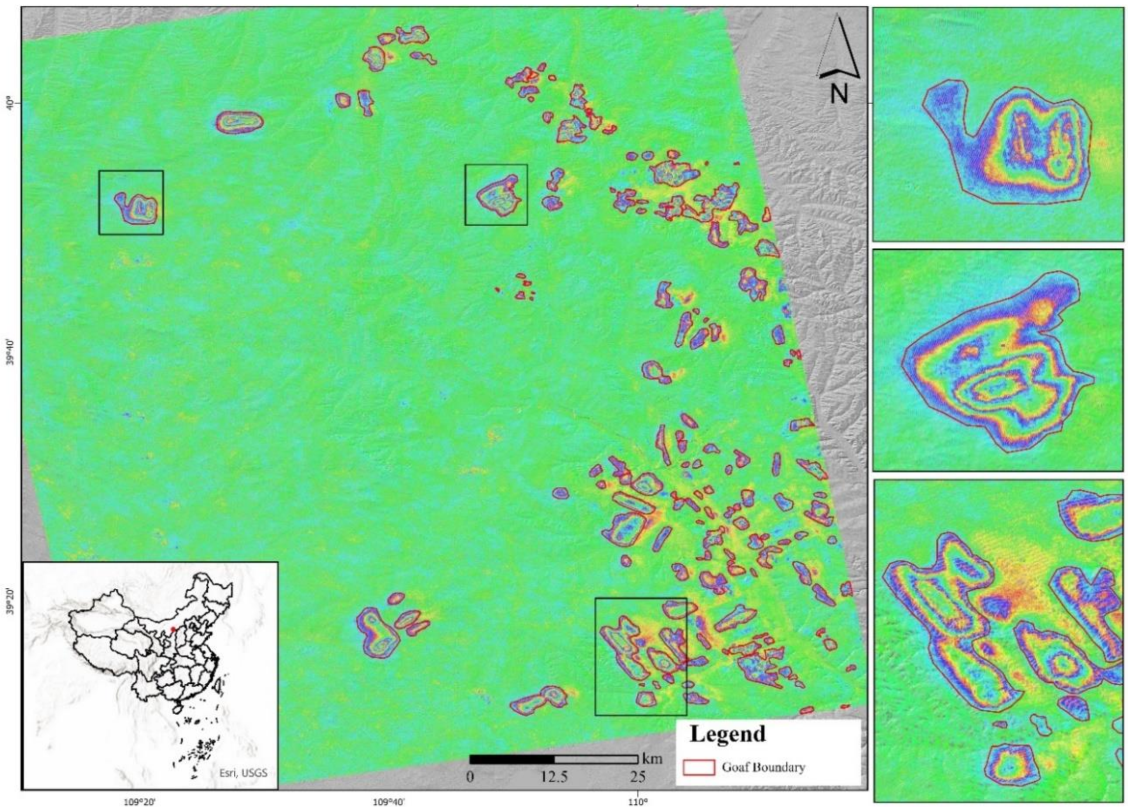

Figure 1. Annual deformation rate of Ordos and enlarged views of typical ereas

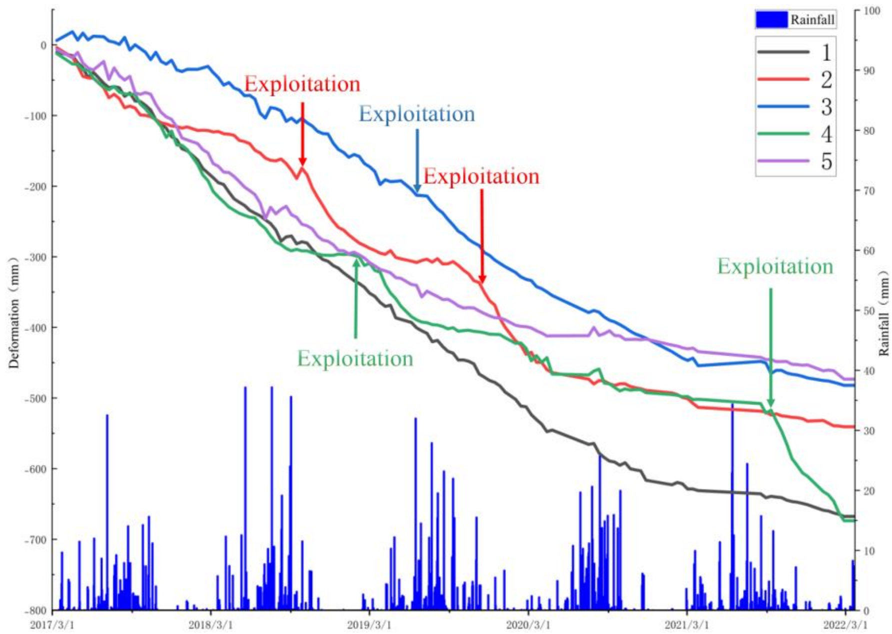

Figure 2. Deformation results from the time series curve of characteristic points in the subsidence zone

Conclusion

To mitigate the threats to personal safety and property loss caused by geological disasters in large subsidence areas resulting from extensive mining activities in Ordos City, it is crucial to accurately determine the subsidence zones within goaf areas.

By analyzing surface deformation rates and distribution patterns, along with temporal analysis of deformation characteristics, these hidden geological dangers can be effectively identified and addressed, reducing the risks associated with subsidence areas.

References

Baek, et al. "Analysis of ground subsidence in coal mining area using SAR interferometry." Geosciences Journal 12 (2008): 277-284.

Du, Yuling, et al. "Investigation of deformation patterns by DS-InSAR in a coal resource-exhausted region with Spaceborne SAR imagery." Journal of Asian Earth Sciences: X 5 (2021): 100049.

Hooper, Andrew, and Howard A. Zebker. "Phase unwrap** in three dimensions with application to InSAR time series." JOSA A 24.9 (2007): 2737-2747.

Li, Lu, et al. "An Automatic Spatial-Temporal Evolution Inversion Method of Mining Goaf Based on the Improved Hotspot Analysis and Probability Integral Method." IEEE Journal of Selected Topics in Applied Earth Observations and Remote Sensing (2023).

Li, Menghua, et al. "Detection of coal-mining-induced subsidence and map** of the resulting deformation using time series of ALOS-PALSAR data." Remote Sensing Letters 7.9 (2016): 855-864.

Liu, Lin, et al. "Accelerated glacier mass loss (2011–2016) over the Puruogangri ice field in the inner Tibetan Plateau revealed by bistatic InSAR measurements." Remote Sensing of Environment 231 (2019): 111241.

Zhang, Yonghong, et al. "Monitoring of urban subsidence with SAR interferometric point target analysis: A case study in Suzhou, China." International Journal of Applied Earth Observation and Geoinformation 13.5 (2011): 812-818.

Zhao, Changjun, et al. "A ground surface deformation monitoring InSAR method using improved distributed scatterers phase estimation." IEEE Journal of Selected Topics in Applied Earth Observations and Remote Sensing 12.11 (2019): 4543-4553.

UNSTABLE SEEPAGE CHARACTERISTICS OF UNDERLYING SOFT CLAY ASSOCIATED WITH MICROSCOPIC MECHANISM IN RECLAMATION AREA: A CASE STUDY

MENG YAO [1], QING WANG [1], QINGBO YU [1], JIANPING CHEN [1]

[1] *College of Construction Engineering, Jilin University, Changchun 130026, China, yuqb@jlu.edu.cn*

Introduction

Artificial reclamation is one of the main means of land expansion for many coastal cities around the world. However, the permeability of underlying soft clay (USC), derived from the dredged load, has not been paid enough attention, although it is closely related to the long-term deformation and stability of foundation soil. Hence, this paper analyzes the relationship between time-varying permeability characteristics and microscopic pore characteristics of USC in reclamation area. This paper may provide a scientific basis for explaining the long-term differential subsidence in different reclamation areas and other similar areas.

Methods

Chongming East Shoal located at the eastern end of Chongming Island, is one of the typical multi-phase reclamations in Shanghai. Five boreholes were arranged from west to east to obtain the property change of soft clay in different reclamation periods.A series of indoor tests, including the variable head permeability test, mercury intrusion porosimetry, and scanning electron microscope, were carried out to reveal the micro-mechanism of differential permeability.

Results

The results revealed that the seepage process of clay showed a transition from unstable seepage to relatively stable seepage. Meanwhile, the permeability coefficient (PC) attenuated with time cyclically, indicating the alternating effect of the closed and opened unstable seepage channels. During seepage, clay particles could be entrained by pore water and intercepted by pores, thus clogging seepage channels. Then, the increased pore water pressure could break through new seepage channels. The degree of pore clogging was positively correlated with the average cycle period of PCs, and this was also present in the relatively stable stage of PCs.

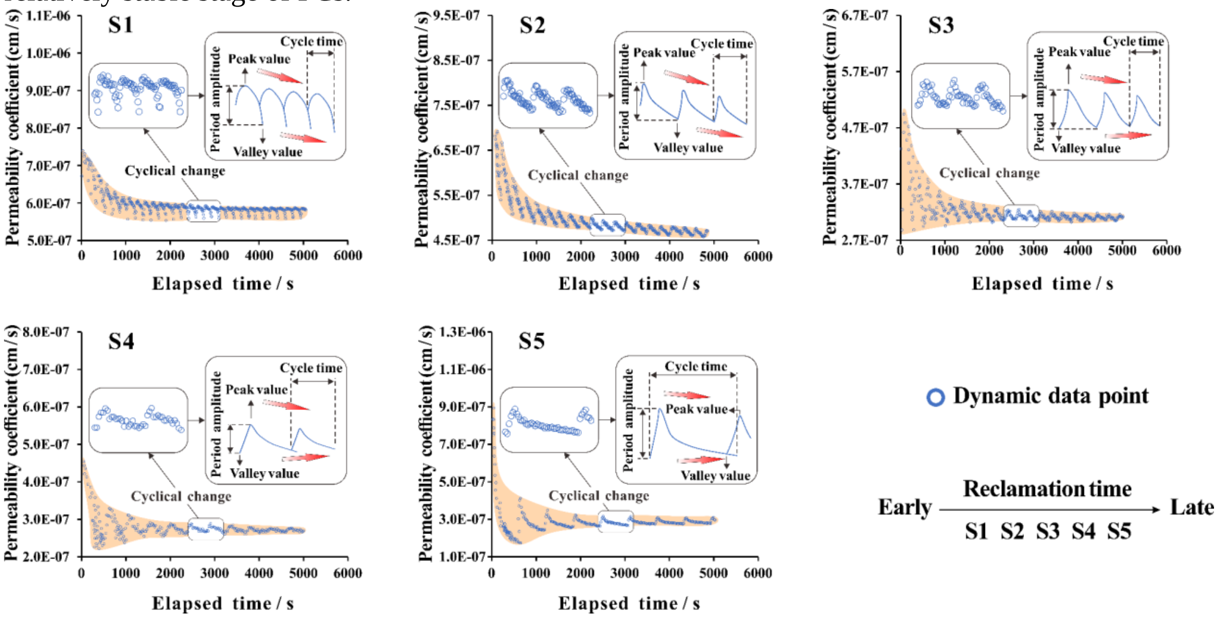

Figure 1. Evolution and statistics (per 1000 s) of representative permeability coefficients of soil samples S1-S5.

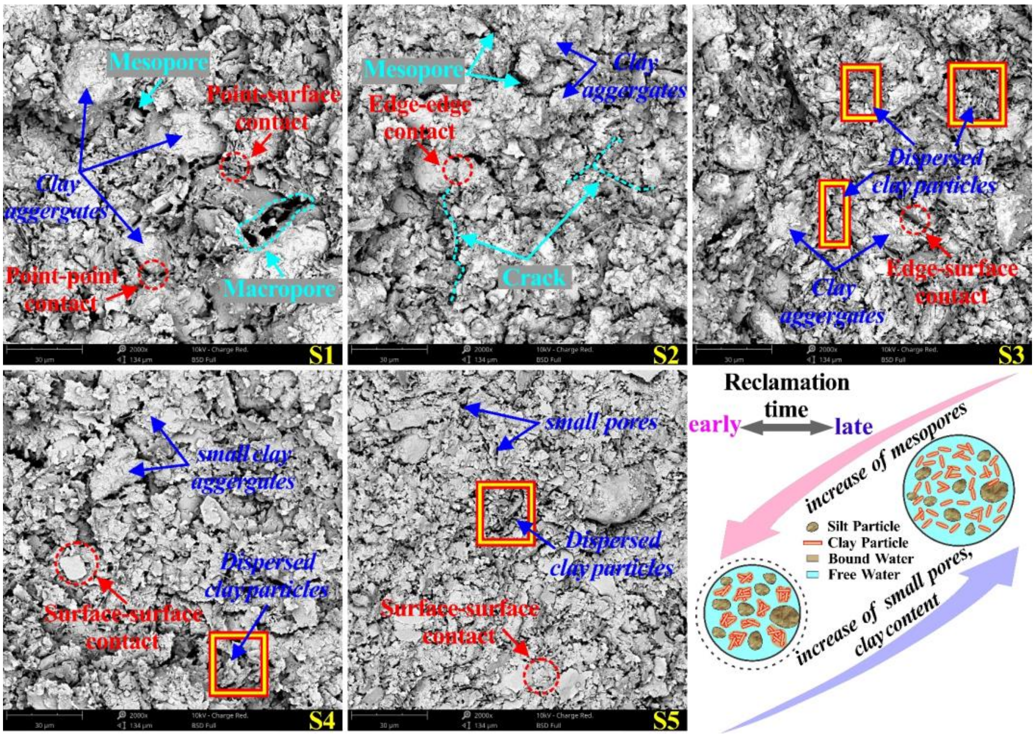

Figure 2. Microstructure characteristics of USC in different reclamation areas

Conclusion

A lower mesopores content, higher fractal dimension, and aggregated flocculate microstructure could promote the clogging effect and result in lower permeability efficiency. Affected by unstable seepage channels, soft clay may face long-term potential deformation in the future, which needs further investigation.

References

Yuan, X.Q.; Wang, Q.; Lu, W.X.; Zhang, W.; Chen, H.E.; Zhang, Y. Indoor simulation test of step vacuum preloading for high-clay content dredger fill. *Marine Georesources & Geotechnology*. 2018, 36, 83–90.

Horikoshi, K.; Takahashi, A. Suffusion-induced change in spatial distribution of fine fractions in embankment subjected to seepage flow. *Soils and Foundations.* 2015, 55, 1293–1304.

Zhang, M.X.; Zhu, X.W.; Yu, G.L.; Yan, J.M.; Wang, X.B.; Chen, M.L.; Wang, W.M. Permeability of muddy clay and settlement sim-ulation. *Ocean Engineering.* 2015, 104, 521–529.

Han, Y.; Wang, Q.; Xia, W.T.; Liu, J.; Wang, J.Q.; Chen, Y.T.; Shen, J.J. Experimental study on the hydraulic conductivity of un-saturated dispersive soil with different salinities subjected to freeze-thaw. *Journal of Hydrology.* 2020, 583, 124297.

HIGH-SPEED IDENTIFICATION OF COMPLEX DISCONTINUITIES IN LARGE-SCALE ROCK OUTCROPS

WEN ZHANG [1], JIALI HAN [2], JIANPING CHEN [3], QING WANG [4]

[1] *Jilin University, China, zhang_wen@jlu.edu.cn*

[2] *Jilin University, China, Jlhan21@mails.jlu.edu.cn*

[3] *Jilin University, China, chenjp@jlu.edu.cn*

[4] *Jilin University, China, wangqing@jlu.edu.cn*

Introduction

Discontinuities on slopes typically exhibit lower mechanical strength compared to the intact rock, making rockfalls and landslides slide along them. As a result, accurately identifying discontinuities on high and steep slopes is crucial for determining the boundaries of engineering geohazards.

Point cloud data is widely used in automatic identification research. Traditional methods for automatic identification based on point cloud data can be broadly classified into two categories: clustering methods and region growing methods. While these algorithms have produced significant results in academic research, previous studies have predominantly focused on simpler scenarios. These scenarios often involve smaller point cloud datasets, and more regularly developed discontinuities with distinct variations among different groups of discontinuities.

In contrast, practical large-scale applications present more challenging conditions, with discontinuities that are numerous, and highly disordered with complex orientations non-smooth surfaces. These complexities place greater demands on the ability of the algorithm to accurately process and efficiently identify discontinuity.

The objective of this paper is to develop an algorithm capable of efficiently processing point clouds containing tens of millions of points while ensuring high recognition accuracy for complex discontinuities.

Methods

This paper proposes an edge-first connection algorithm, which first identifies all discontinuity edge points in the point cloud without considering their specific association with any particular discontinuity. The next step is to merge the non-edge points belonging to the same discontinuity through a connectivity operation, thereby completing the identification process. This approach differs from traditional algorithms that sequentially identify one discontinuity at a time before moving on to the next. The advantage of the edge-first connection algorithm is that it simplifies complex logical operations during computation, significantly improving computational efficiency.

The first step of the proposed method based on point cloud data is to identify discontinuity edges within the neighbourhood. The method identifies edge points by analyzing the deviation of normal vectors. Specifically, the normal vector for each point is calculated by fitting a plane to its nearest neighbouring points. If the angle between the normal vector of a point and its neighbours exceeds a set threshold, the point is classified as an edge point. This process is repeated for all points, effectively identifying the edge points in the point cloud.

The second step of the method involves merging non-edge points belonging to the same discontinuity by checking for shared neighbouring points. Closely located non-edge points within the same discontinuity tend to have overlapping neighbourhoods, while points from different discontinuities do not share neighbours due to edge points separating them. This process is facilitated by applying connectivity principles from graph theory, where points and their neighbours are treated as subsets of nodes. The algorithm identifies and merges connected subsets until it forms maximal connected subsets, representing complete discontinuities.

Results

The edge-first connection algorithm was applied to identify discontinuities on the Xulong slope located in the Jinsha River suture zone. The slope, measuring 280 meters in length and 200 meters in height, comprises a point cloud with 13 million points. The algorithm efficiently identified 2780 discontinuities on the slope within just 3 hours, demonstrating excellent recognition efficiency. A comparison between the discontinuities identified by the automatic method and those identified manually on the model revealed that the pole plots from both methods had highly similar pole distributions and high-density centres (Figure 1). Furthermore, both methods identified three dominant groups of discontinuities, with their orientations shown in Table 1. The differences in orientations between the dominant groups identified by the two methods ranged from 2° to 8°. This result demonstrates that the edge-first connection algorithm also delivers highly satisfactory accuracy in recognizing complex fractures over large areas.

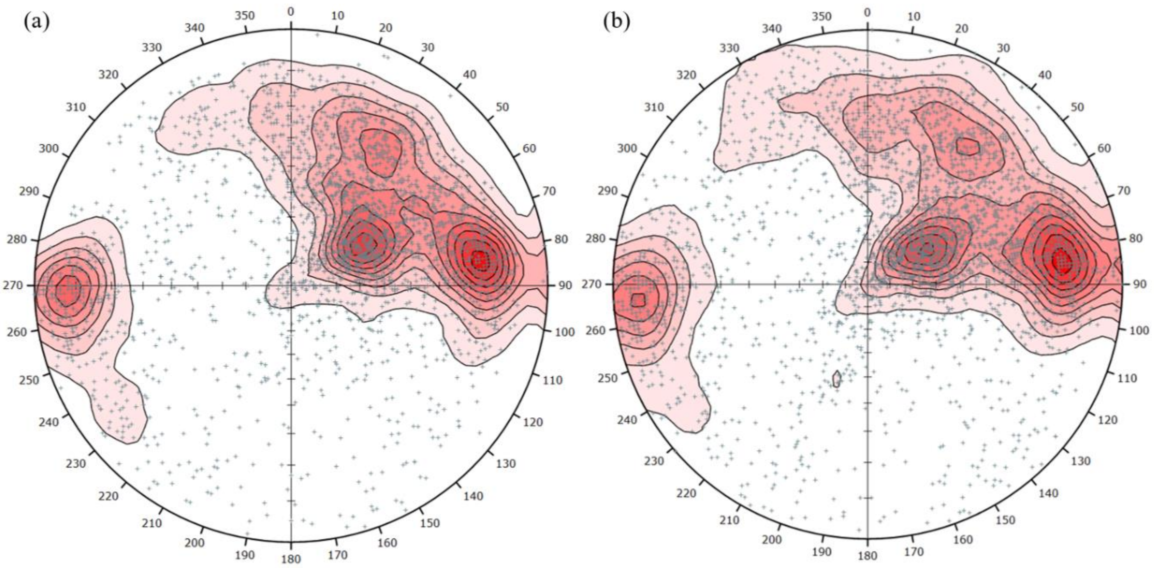

Figure 1. The comparison of pole charts from automatic method (a) and manual method (b).

Table 1. The comparison of the dominant groups from automatic and manual method

Method	Group 1	Group 2	Group 3
Automatic	46°∠30°	84°∠74°	23°∠63°
Manual	51°∠32°	76°∠72°	20°∠60°

Conclusion

This paper presents an edge-first connection algorithm that uses a computational approach distinct from traditional methods, significantly reducing complex logical operations. When applied to identifying discontinuities on the Xulong slope in the Jinsha River suture zone, the algorithm delivered outstanding results, showcasing both high computational efficiency and impressive accuracy. These outcomes demonstrate the feasibility of rapidly identifying complex discontinuities across large-scale rock slopes.

References

Assali, P., Grussenmeyer, P., Villemin, T., Pollet, N. & Viguier, F. Surveying and modeling of rock discontinuities by terrestrial laser scanning and photogrammetry: Semi-automatic approaches for linear outcrop inspection. Journal of Structural Geology. 2014, 66:102-114.

Battulwar, R., Zare-Naghadehi, M., Emami, E. & Sattarvand, J. A state-of-the-art review of automated extraction of rock mass discontinuity characteristics using three-dimensional surface models. Journal of Rock Mechanics and Geotechnical Engineering. 2021, 13(4):920-936.

Brideau, M.-A., Yan, M. & Stead, D. (2009) The role of tectonic damage and brittle rock fracture in the development of large rock slope failures. Geomorphology. 2009, 103(1):30-49.

Chen, J., Zhu, H. & Li, X. Automatic extraction of discontinuity orientation from rock mass surface 3D point cloud. Computers & Geosciences. 2016, 95:18-31.

Chen, N., Cai, X., Li, S., Zhang, X. & Jiang, Q. Automatic extraction of rock mass discontinuity based on 3D laser scanning. Quarterly Journal of Engineering Geology and Hydrogeology. 2020, 54(1):qjegh2020-054.

Daghigh, H., Tannant, D. D., Daghigh, V., Lichti, D. D. & Lindenbergh, R. A critical review of discontinuity plane extraction from 3D point cloud data of rock mass surfaces. Computers & Geosciences. 2022, 169:105241.

Ding, L., Kapp, P. & Wan, X. Paleocene-Eocene record of ophiolite obduction and initial India-Asia collision, South central Tibet. Tectonics. 2005, 24:TC3001.

Drews, T., Miernik, G., Anders, K., Höfle, B., Profe, J., Emmerich, A. & Bechstädt, T. Validation of fracture data recognition in rock masses by automated plane detection in 3D point clouds. International Journal of Rock Mechanics and Mining Sciences. 2018, 109:19-31.

Ferrero, A. M., Forlani, G., Roncella, R. & Voyat, H. I. (2009) Advanced Geostructural Survey Methods Applied to Rock Mass Characterization. Rock Mechanics and Rock Engineering. 2009, 42(4):631-665.

Ge, Y., Cao, B. & Tang, H. (2022) Rock Discontinuities Identification from 3D Point Clouds Using Artificial Neural Network. Rock Mechanics and Rock Engineering. 2022, 55(3):1705-1720.

Ge, Y., Tang, H., Xia, D., Wang, L., Zhao, B., Teaway, J. W., Chen, H. & Zhou, T. Automated measurements of discontinuity geometric properties from a 3D-point cloud based on a modified region growing algorithm. Engineering Geology. 2018, 242:44-54.

Gigli, G. & Casagli, N. Semi-automatic extraction of rock mass structural data from high resolution LIDAR point clouds. International Journal of Rock Mechanics and Mining Sciences. 2011, 48(2):187-198.

Gomes, R. K., De Oliveira, L. P. L., Gonzaga, L., Tognoli, F. M. W., Veronez, M. R. & De Souza, M. K. An algorithm for automatic detection and orientation estimation of planar structures in LiDAR-scanned outcrops. Computers & Geosciences. 2016, 90:170-178.

Hu, L., Xiao, J. & Wang, Y. Efficient and automatic plane detection approach for 3-D rock mass point clouds. Multimedia Tools and Applications. 2020, 79(1):839-864.

Kong, D., Wu, F. & Saroglou, C. Automatic identification and characterization of discontinuities in rock masses from 3D point clouds. Engineering Geology. 2020, 265:105442.

Menegoni, N., Giordan, D., Perotti, C. & Tannant, D. D. Detection and geometric characterization of rock mass discontinuities using a 3D high-resolution digital outcrop model generated from RPAS imagery–Ormea rock slope, Italy. Engineering Geology. 2019, 252:145-163.

Olariu, M. I., Ferguson, J. F., Aiken, C. L. V. & Xu, X. Outcrop fracture characterization using terrestrial laser scanners: Deep-water Jackfork sandstone at Big Rock Quarry, Arkansas. Geosphere. 2008, 4(1):247-259.

Riquelme, A., Cano, M., Tomás, R. & Abellán, A. Identification of Rock Slope Discontinuity Sets from Laser Scanner and Photogrammetric Point Clouds: A Comparative Analysis. Procedia Engineering. 2017, 191:838-845.

Riquelme, A. J., Abellán, A., Tomás, R. & Jaboyedoff, M. A new approach for semi-automatic rock mass joints recognition from 3D point clouds. Computers & Geosciences. 2014, 68:38-52.

Singh, S. K., Raval, S. & Banerjee, B. P. Automated structural discontinuity mapping in a rock face occluded by vegetation using mobile laser scanning. Engineering Geology. 2021, 285:106040.

Sturzenegger, M. & Stead, D. Close-range terrestrial digital photogrammetry and terrestrial laser scanning for discontinuity characterization on rock cuts. Engineering Geology. 2009, 106(3):163-182.

Sun, W., Wang, J., Yang, Y. & Jin, F. Rock Mass Discontinuity Extraction Method Based on Multiresolution Supervoxel Segmentation of Point Cloud. IEEE Journal of Selected Topics in Applied Earth Observations and Remote Sensing. 2021, PP:1-1.
Wang, S., Zhang, W., Zhao, X., Sun, Q. & Dong, W. Automatic identification and interpretation of discontinuities of rock slope from a 3D point cloud based on UAV nap-of-the-object photogrammetry. International Journal of Rock Mechanics and Mining Sciences. 2024, 178:105774.
Wang, W., Zhao, W., Chai, B., Du, J., Tang, L. & Yi, X. Discontinuity interpretation and identification of potential rockfalls for high-steep slopes based on UAV nap-of-the-object photogrammetry. Computers & Geosciences. 2022, 166:105191.
Wang, X., Zou, L., Shen, X., Ren, Y. & Qin, Y. A region-growing approach for automatic outcrop fracture extraction from a three-dimensional point cloud. Computers & Geosciences. 2017, 99:100-106.
Wasantha, P. L. P., Ranjith, P. G., Xu, T., Zhao, J. & Yan, Y. L. (2014) A new parameter to describe the persistency of non-persistent joints. Engineering Geology. 2014, 181:71-77.
Wilkinson, M. W., Jones, R., Woods, C. E., Gilment, S., Mccaffrey, K., Kokkalas, S. & Long, J. A comparison of terrestrial laser scanning and structure-from-motion photogrammetry as methods for digital outcrop acquisition. Geosphere. 2016, 12:GES01342.1.
Wu, Q. & Kulatilake, P. H. S. W. (2012) REV and its properties on fracture system and mechanical properties, and an orthotropic constitutive model for a jointed rock mass in a dam site in China. Computers and Geotechnics. 2012, 43:124-142.
Wu, Q., Liu, Y., Tang, H., Kang, J., Wang, L., Li, C., Wang, D. & Liu, Z. Experimental study of the influence of wetting and drying cycles on the strength of intact rock samples from a red stratum in the Three Gorges Reservoir area. Engineering Geology. 2023, 314:107013.
Yan, J., Chen, J., Zhan, J., Song, S., Zhang, Y., Zhao, M., Liu, Y. & Xu, W. Automatic identification of rock discontinuity sets using modified agglomerative nesting algorithm. Bulletin of Engineering Geology and the Environment. 2022, 81(6):229.
Yi, X., Feng, W., Wang, D., Yang, R., Hu, Y. & Zhou, Y. An efficient method for extracting and clustering rock mass discontinuities from 3D point clouds. Acta Geotechnica. 2023, 18(7):3485-3503.
Zeng, Y., Lei, Q., Wang, Z., Ding, S., Liu, K., Huang, X., Huang, Z. & Wang, X. Numerical simulation of fluid injection-induced fault slip in heterogeneous shale formations. Computers and Geotechnics. 2021, 134:104120.
Zhang, S.-L., Yin, Y.-P., Hu, X.-W., Wang, W.-P., Zhu, S.-N., Zhang, N. & Cao, S.-H. Initiation mechanism of the Baige landslide on the upper reaches of the Jinsha River, China. Landslides. 2020, 17:2865-2877.
Zhang, W., Han, J., Lu, C., Liu, H., Chen, J., Wang, J., Li, T. & Chen, J. Geometric searching of 3D critical slip surface of a non-persistent fracture-dominated rock slope. Computers and Geotechnics. 2024, 173:106493.
Zhang, W., Zhao, X., Pan, X., Wei, M., Yan, J. & Chen, J. Characterization of high and steep slopes and 3D rockfall statistical kinematic analysis for Kangyuqu area, China. Engineering Geology. 2022, 308:106807.